Regd. No. C-3911

VOL. 35

INDIAN JOURNAL OF PHYSICS

No. 7

(Published in collaboration with the Indian Physical Society)

AND

VOL. 44

PROCEEDINGS

No. 7

OF THE

INDIAN ASSOCIATION FOR THE CULTIVATION OF SCIENCE

JULY 1961

PUBLISHED BY THE

INDIAN ASSOCIATION FOR THE CULTIVATION OF SCIENCE

JADAVPUR, CALCUTTA 32

Annual Subscription—
Inland Rs. 25.00
Foreign £ 2-10-0 or $ 7.00

NOTICE
TO INTENDING AUTHORS

1. Manuscripts for publication should be sent to the Assistant Editor, Indian Journal of Physics, Jadavpur, Calcutta-32.

2. The manuscripts submitted must be type-written with double space on thick foolscap paper with sufficient margin on the left and at the top. The original copy, and not the carbon copy, should be submitted. Each paper must contain an Abstract at the beginning.

3. All References should be given in the text by quoting the surname of the author, followed by year of publication, *e.g.*, (Roy, 1958). The full Reference should be given in a list at the end, arranged alphabatically, as follows; Mazumder, M. 1959, *Ind. J. Phys.*, **33**, 346.

4. Line diagrams should be drawn on white Bristol board or tracing paper with black Indian ink, and letters and numbers inside the diagrams should be written neatly in capital type with Indian ink. The size of the diagrams submitted and the lettering inside should be large enough so that it is legible after reduction to one-third the original size. A simple style of lettering such as gothic, with its uniform line width and no serifs should be used, *e.g.*,

A·B·E·F·G·M·P·T·W·

5. Photographs submitted for publication should be printed on glossy paper with somewhat more contrast than that desired in the reproduction.

6. Captions to all figures should be typed in a separate sheet and attached at the end of the paper.

7. The mathematical expressions should be written carefully by hand. Care should be taken to distinguish between capital and small letters and superscripts and subscripts. Repetition of a complex expression should be avoided by representing it by a symbol. Greek letters and unusual symbols should be identified in the margin. Fractional exponents should be used instead of root signs.

36

MICROWAVE ANALOGUE FOR X-RAY DIFFRACTION PART II. SIZE OF THE SCATTERERS

G. S. SANYAL AND G. B. MITRA

INDIAN INSTITUTE OF TECHNOLOGY, KHARAGPUR

(*Received March* 8, 1961)

ABSTRACT. The variation with the azimuthal angle of scattering of amplitude of electromagnetic waves scattered by conducting spheres of sizes (a) comparable and (b) negligible with respect to the wave-length has been studied. A workable theoretical expression has been obtained and evaluated by carrying out numerical computations. The theoretical expressions to be computed contain high order Hankel functions, Legendre polynomials and their derivatives numerical values of which are not given in ordinarily available tables. These values have been calculated and used in the numerical computations. The resultant curves show that the conducting sphere with $2\pi a/\lambda = 2$, where 'a' is the radius of the sphere and λ the wavelength of the e.m. waves is the nearest approximation to several atoms as far as scattering behaviour towards X-rays is concerned.

I. INTRODUCTION

Recently, Allen (1955) and Mitra and Sanyal (1960) have studied the scattering of electromagnetic waves in the microwave region by three dimensional arrays of metallic scatterers. While Allen (1955) worked with metallic discs as scatterers, Mitra and Sanyal (1960) used small cylinders for the purpose. Such scatterers, however, can hardly be used to build a true analogue in the microwave region for the diffraction of X-rays by crystals. The scatterers which are meant to simulate the atoms in the crystal lattices lack the spherical or near spherical symmetry possessed by atoms. Moreover, the variation of amplitude of electromagnetic waves scattered by these scatterers with the azimuthal angle of scattering should be similar to the atomic scattering factor graphs to make the analogue serve any useful purpose. It appears obvious that a solid sphere of dielectric or conducting material and of a proper size should serve the purpose, more or less, adequately. Hence, it has been decided to investigate theoretically the scattering patterns of conducting spheres to find out the proper size whose scattering pattern will approximate to the atomic scattering factor graphs. Since ionic radii of atoms are of the order of X-ray wavelengths, it has been intuitively felt that the proper size of the diffracting sphere would probably be comparable to the wavelength used. The case of vanishing sphere-size has also been studied to investigate the effect of diminishing the sphere-size.

Although the problem of diffraction of electromagnetic waves by spheres and spheroids has been studied by various authors [Mie, (1908), Blumer (1925, 1926a,

1926b and 1926c)] investigations of the type envisaged by us have not been carried out so far. Hence it has been decided to plot the graphs of the amplitude of microwaves scattered by spheres against the azimuthal angle of scattering for conducting spheres of sizes given by $\rho = 6$, $\rho = 2$ and $\rho \to 0$ where $\rho = 2\pi a/\lambda$, 'a' being the radius of the sphere and λ the wavelength used. Only conducting spheres have been considered to render the already formidable numerical computations somewhat less complicated.

II. THEORETICAL CONSIDERATIONS

Let a plane electromagnetic wave, propagating in free-space along the z-axis and polarised linearly along the x-axis, be incident on a *perfectly conducting sphere* of radius 'a' located at the origin of a spherical co-ordinate system r, θ, ϕ as shown in Fig. 1. The scattering process will be such that the resultant electromagnetic field satisfies the boundary conditions on the surface of the sphere and also reduces to a plane wave at a large distance r. The expressions for the scattered electromagnetic fields have been given by Stratton (1941). Thus for an incident plane electromagnetic wave expressed as

$$\bar{E}_i = \bar{1}_x E_0 \exp i(\beta z - \omega t)$$

$$\bar{H}_i = \bar{1}_y (E_0/\sqrt{\mu_0/\epsilon_0}) \exp i(\beta z - \omega t),$$

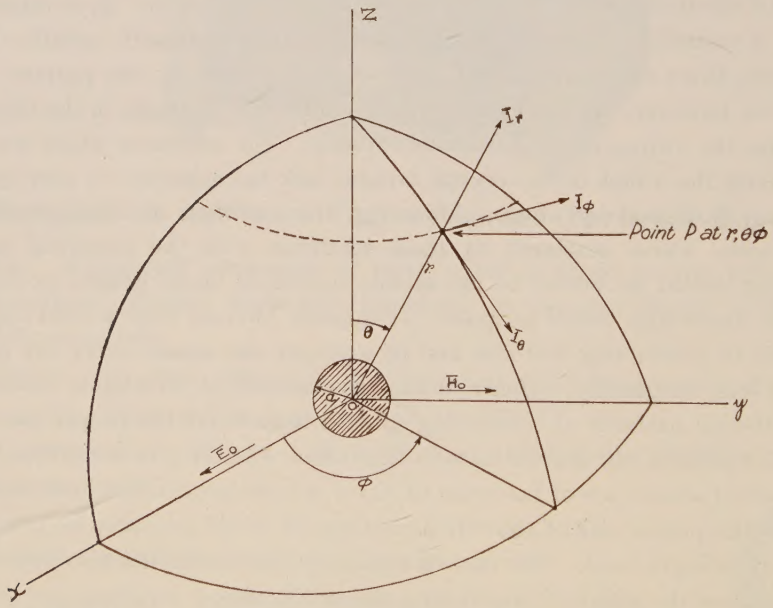

Fig. 1. Conducting sphere of radius 'a' located at the origin of a spherical coordinate system. $\bar{1}_r$, $\bar{1}_\theta$, $\bar{1}_\varphi$ are mutually orthogonal unit vectors at the point P.

the scattered electric field vector at any point $P(r, \theta, \phi)$ outside the sphere is

$$\bar{E}_S = E_0 \exp(-i\omega t) \sum_{n=1}^{\infty} i^n \frac{2n+1}{n(n+1)} [a^S{}_n \bar{m}_{01n} - i\, b^S{}_n \bar{n}_{e1n}] \quad \ldots \quad (1)$$

where, E_0 is the amplitude of the incident electric field

β, the phase constant of the plane wave in free-space $= \omega\sqrt{\mu_0\epsilon_0} = 2\pi/\lambda_0$,

λ_0 being the free-space wavelength

μ_0, the permeability of free-space $= 1.257 \times 10^{-6}$ H/metre

ϵ_0, the permittivity of free-space $= 8.854 \times 10^{-12}$ F/metre

$\omega = 2\pi f$, f being the frequency of the incident wave

$\bar{m}_{01n}$, an odd vector function

$$= \bar{1}_\theta \left[\frac{1}{\sin\theta} h^{(1)}{}_n(\beta r) P^1{}_n (\cos\theta) \cos\phi \right]$$

$$- \bar{1}_\varphi \left[h^{(1)}{}_n(\beta r) \frac{\partial P^1{}_n (\cos\theta)}{\partial\theta} \sin\phi \right]$$

$\bar{n}_{e1n}$ an even vector function

$$= \bar{1}_r \left[\frac{n(n+1)}{\beta r} h^{(1)}{}_n(\beta r) P^1{}_n (\cos\theta) \cos\phi \right]$$

$$+ \bar{1}_\theta \left[\frac{1}{\beta r} \frac{\partial\{\beta r h^{(1)}{}_n(\beta r)\}}{\partial(\beta r)} \frac{\partial P_n{}^1(\cos\theta)}{\partial\theta} \cos\phi \right]$$

$$- \bar{1}_\phi \left[\frac{1}{\beta r \sin\theta} \frac{\partial\{\beta r h_n{}^{(1)}(\beta r)\}}{\partial(\beta r)} P^1{}_n (\cos\theta) \sin\phi \right]$$

$$a^S{}_n = -j_n(\rho)/h^{(1)}{}_n(\rho)$$

$$b^S{}_n = -\left[\frac{d}{d\rho} \{\rho j_m(\rho)\} \right] \Big/ \left[\frac{d}{d\rho} \{\rho h^{(1)}{}_n(\rho)\} \right]$$

$$j_n(\rho) = \sqrt{(\pi/2\rho)}\ J_{n+\frac{1}{2}}(\rho)$$

$$h^{(1)}{}_n(\rho) = \sqrt{(\pi/2\rho)}\ H^{(1)}{}_{n+\frac{1}{2}}(\rho)$$

$$\rho = 2\pi a/\lambda$$

$J_{n+\frac{1}{2}}$ and $H^{(1)}{}_{n+\frac{1}{2}}$ are respectively Bessel and first kind Hankel functions each of order $n+\frac{1}{2}$

$P^1{}_n$ $(\cos\theta)$ is an associated Legendre polynomial.

The theoretical scattering pattern at a very large distance away from the conducting sphere may now be calculated from Eq.(1). The form given by Morse and Feshbach (1953) requires to be further simplified for direct computation and will not be used in this article. It is enough for our purpose to consider the variation of the electric field vector alone, since at a large distance the scattered field reduces to a uniform plane wave. The simplified asymptotic form of Eq. (1) valid at a large distance i.e. $\beta r >> 1$ and $r >> a$ may be arrived at by noting that

$$\text{Lim.}_{\beta r>>1}\, h_n^{(1)}(\beta r) \rightarrow \frac{1}{\beta r}\ (-i)^{n+1} \exp(i\beta r)$$

$$\text{Lim}_{\beta r>>1}\ \frac{1}{\beta r}\ \frac{d\{\beta r h_n^{(1)}(\beta r)\}}{d(\beta r)} \rightarrow \frac{1}{\beta r}\ (-i)^n \exp(i\beta r).$$

Substitution of the limiting values of the above two expressions in Eq.(1) yields the components of the scattered electric field vector at a large distance as

$$E_{Sr} = 0$$

$$E_{S\theta} = -\frac{iE_0 \cos\phi}{\beta r} \exp\ i(\beta r - \omega t) \times$$

$$\sum_{n=1}^{\infty} \frac{2n+1}{n(n+1)} \left[a_n{}^S \frac{P_n{}^1(\cos\theta)}{\sin\theta} + b_n{}^S \frac{dP_n{}^1(\cos\theta)}{d\theta} \right]$$

$$E_{S\varphi} = \frac{iE_0 \sin\phi}{\beta r} \exp\ i(\beta r - \omega t) \times$$

$$\sum_{n=1}^{\infty} \frac{2n+1}{n(n+1)} \left[a_n{}^S \frac{dP_n{}^1(\cos\theta)}{d\theta} + b_n{}^S \frac{P_n{}^1(\cos\theta)}{\sin\theta} \right] \qquad \ldots (2)$$

The rate of convergence of the above expressions for the θ and ϕ components of the scattered field depends largely upon the convergence of $a_n{}^S$ and $b_n{}^S$ for successively increasing values of n. For values of ρ *large* compared to unity, both the terms inside the square brackets of Eq.(2) converge very slowly and the

summation has to be carried out over a large value of n. In the special case when ρ is *finite* but very much less than unity, $a_n{}^S$ and $b_n{}^S$ can be expanded in powers of ρ giving to the first order of approximation

$$b_n{}^S \simeq -\frac{2}{3} i\rho^3 \quad \text{for} \quad n=1$$

$$\simeq 0 \quad \text{for} \quad n>1$$

$$a_n{}^S \simeq \frac{1}{3} i\rho^3 \quad \text{for} \quad n=1$$

$$\simeq 0 \quad \text{for} \quad n>1$$

Substitution of these values of $a_n{}^S$ and $b_n{}^S$ in Eq. (2) yields the scattered fields in the far zone due to a *finite but very small* conducting sphere as

$$E_{S\theta} = \frac{1}{2} \frac{E_0 \cos\phi}{\beta r} \rho^3(1-2\cos\theta) \exp i(\beta r-\omega t)$$

$$= \frac{2\pi^2 E_0 \cos\phi}{\lambda^2 r} a^3(1-2\cos\theta) \exp i(\beta r-\omega t)$$

$$E_{S\varphi} = \frac{1}{2} \frac{E_0 \sin\phi}{\beta r} \rho^3(2-\cos\theta) \exp i(\beta r-\omega t)$$

$$= \frac{2\pi^2 E_0 \sin\phi}{\lambda^2 r} a^3(2-\cos\theta) \exp i(\beta r-\omega t) \quad \ldots \quad (3)$$

III. NUMERICAL COMPUTATION

To study the nature of the variation of the scattered field with the polar angle θ, the summation in Eq. (2) has to be performed over a sufficiently large value of n. In this article n has been so chosen that the numerical result may be correct to, at least, the third decimal place. Numerical computation for only $E_{S\varphi}$ and that too for three values of ρ, (i) $\rho << 1$ i.e., $a << \lambda$, (ii) $\rho = 2$ i.e., $a = \lambda/\pi$ and (iii) $\rho = 6$ i.e., $a \simeq \lambda$ has been carried out, since these results are singificant enough to indicate the general nature of variation of the scattered fields with θ and also to show the effect of the radius of the sphere on the scattering pattern. The first case e.g. $\rho < 1$ has been calculated using Eq. (3) and the other two cases by using Eq. (2).

Calculation of the coefficients $a_n{}^S$ and $b_n{}^S$ in Eq.(2) requires tables of j_n and $h_n{}^{(1)}$ functions and their derivatives. Since these tables are not available the coefficients were obtained as follows :

$$a_n{}^S = -\frac{j_n(\rho)}{h_n{}^{(1)}(\rho} = -\frac{J_{n+\frac{1}{2}}(\rho)}{H_{n+\frac{1}{2}}{}^{(1)}(\rho)}$$

$$b_n^S = -\left[\frac{d}{d\rho}\{\rho j_n(\rho)\}\right] \Big/ \left[\frac{d}{d\rho}\{\rho h_n^{(1)}(\rho)\}\right]$$

$$= -\frac{J_{n+\frac{1}{2}}(\rho)+\rho[J_{(n-1)+\frac{1}{2}}(\rho)-J_{(n+1)+\frac{1}{2}}(\rho)]}{H_{n+\frac{1}{2}}^{(1)}(\rho)+\rho[H_{(n-1)+\frac{1}{2}}^{(1)}(\rho)-H_{(n+1)+\frac{1}{2}}^{(1)}(\rho)]}$$

The Hankel function $H_\nu^{(1)}$ itself was computed from the formula

$$H_\nu^{(1)}(x) = [J_{-\nu}(x)-J_\nu(x)\ \exp\ (-\nu\pi i)]/[i \sin \nu\pi]$$

and the tables for J_ν and $J_{-\nu}$ as given by Watson (1922).

Again the numerical computation of Eq.(2) requires the use of the tables of $P_n^1(\cos\theta)$ and its derivate for different values of n. Since these tables also are not available for large n, their values were computed and tabulated for the value of the order n up to 10 by using the recurrence relations :

$$P_{n+1}^1(\cos\theta) = [(2n+1)\cos\theta\, P_n^1(\cos\theta)-(n+1)P_{n-1}^1(\cos\theta)]/n$$

$$d/d\theta[P_n^1(\cos\theta)] = [nP_{n+1}^1(\cos\theta)-(n+1)\cos\theta\, P_n^1(\cos\theta)]/\sin\theta$$

from the lower order polynomials given by Jahnke and Emde (1943).

Eq.(2) can now be evaluated term by term for successively increasing values of n and the summation obtained.

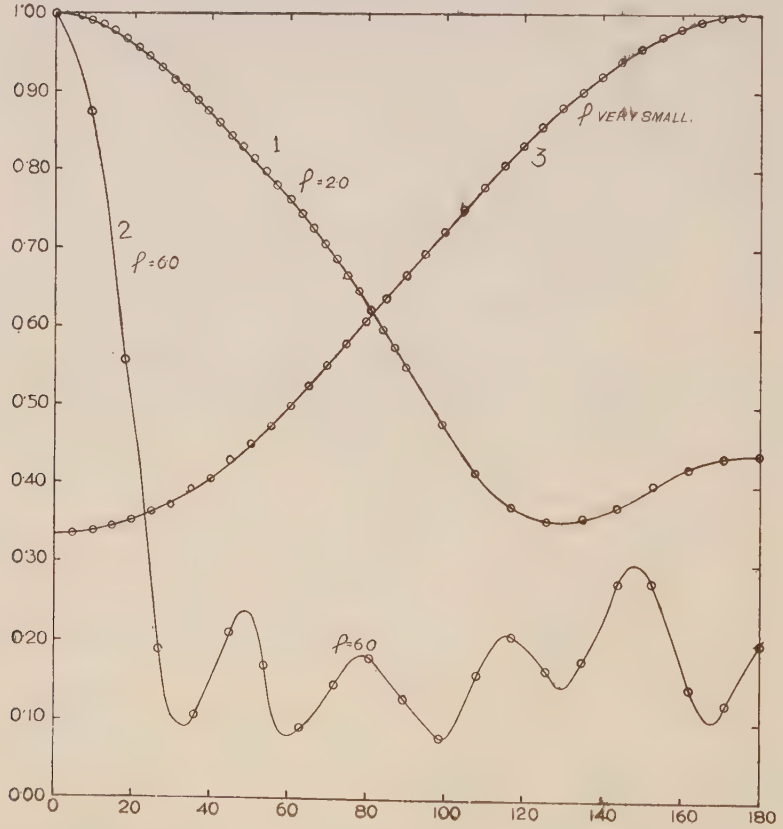

Fig. 2. Scattering patterns of conducting spheres of several sizes (Curve 1, $\rho = 2.0$, Curve 2, $\rho = 6.0$ and Curve 3, ρ very small).

IV. DISCUSSIONS

The theoretical scattering patterns for conducting spheres as computed for the three cases mentioned before are plotted graphically in Fig. 2. Since for each case the relative variation of the scattered field amplitude is of interest, the maximum value of the amplitude has been taken to be equal to 1.00. The scattering patterns show that for the cases when the radius of the sphere is comparable to λ the amplitude gradually decreases with the scattering angle θ. For $\rho = 6$, the curve rapidly decreases from a maximum at $\theta = 0°$ to a minimum at $\theta \simeq 35°$ after which the curve becomes oscillating. For $\rho = 2$, the amplitude falls from a maximum at $\theta = 0°$ almost exponentially till $\theta = 135°$ when there is a tendency to rise rather slowly. The curve for $\rho \to 0$ shows that the scattered amplitude gradually increases with θ. Thus, the sphere with $\rho = 2$ is found to behave, of the three cases considered, in a way nearest to that of atoms as far as the scattering curve is concerned. Fig. 3 shows the variations of amplitude of

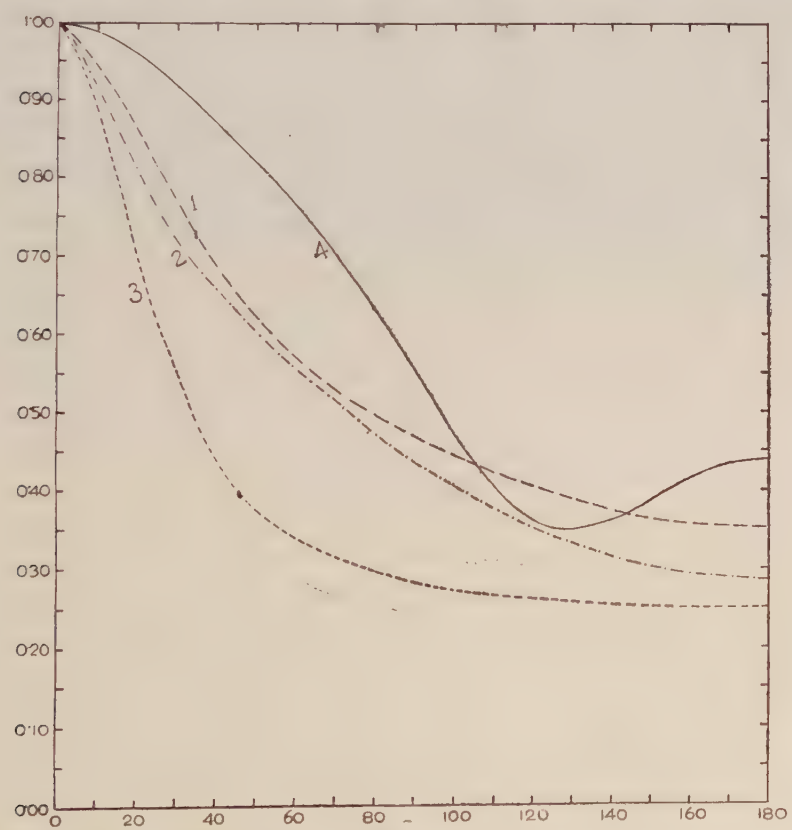

Fig. 3. Variation of the amplitude of X-rays scattered by atoms of copper, aluminium and carbon. Curve 1–copper, Curve 2–aluminium, Curve 3–carbon, Curve 4–scattering pattern of conducting sphere for $\rho = 2.0$.

X-rays scattered by atoms of copper, aluminium and carbon (James and Brinedly, 1931) and for e.m. waves for a conducting sphere with $\rho = 2$. It is observed that the nature of all these curves agree to a large extent. Prehaps better agreement can be achieved with values of ρ which are near to but not exactly equal to 2 or perhaps spheres with different dielectric constants will give better agreement. These cases have not been investigated by us as yet. However, we may safely conclude that with conducting spheres, ρ must have a value very nearly equal to 2 so that the atoms are adequately simulated as far as scattering behaviour is concerned.

REFERENCES

Allen, R. A., 1955, *Am. J. Phys.*, **23**, 297

Blumer, H., 1925, *Z. Physik*, **32**, 119

Blumer, H., 1926a, *Z. Physik*, **38**, 304

Blumer, H., 1926b, *Z. Physik*, **38**, 920

Blumer, H., 1926c, *Z. Physik*, **39**, 195

Jahnke, E. and Emde, F., 1943, Tables of Functions, Dover Publications, New York.

James, B. W., and Brindley, G. W., 1931, *Phil. Mag.*, **12**, 81.

Mie, G., 1908, *Ann. Physik.*, **25**, 377.

Mitra, G. B. and Sanyal, G. S., 1960, *Ind. J. Phys.*, **34**, 103.

Morse, P. M. and Feshback, H., 1953, Methods of Theoretical Physics, Mc-Graw Hill, 1882.

Stratton, J. A., 1941, Electromagnetic Theory, Mc-Graw Hill, 564.

Watson, G. H., 1922, A Treatise on the Theory of Bessel Functions, Cambridge University Press.

37

POTENTIAL FUNCTION OF HELIUM-LIKE ATOMS AND ELECTRON SCATTERING BY THE BORN APPROXIMATION

S. C. MUKHERJEE

Department of Theoretical Physics
Indian Association for the Cultivation of Science,
Jadavpur, Calcutta-32

(*Received March* 30, 1961)

ABSTRACT. In this paper the potential function of helium-like atoms has been derived by using the wave function of Hartree and Ingman (1933) and the scattering cross section of electron by the helium like atoms has been calculated by the method of Born approximation. The theoretical results at low angular range are found to be in excellent agreement with the experimental findings of Hughes, McMillen and Webb (1932).

INTRODUCTION

In calculating the energy eigen values of helium-like atoms by the variational methods the trial wave function has often been chosen as a product of two functions i.e. $f(r_1) \cdot f(r_2)$, where r_1 and r_2 are the position vectors of the two electrons with respect to the nucleus as origin (c.f. Huzinaga, 1960). This type of wave function makes the calculation simple, however, from physical grounds we would expect some dependence of the wave function on r_{12}, the mutual distance between the two electrons. Therefore the simple wave function $f(r_1)\, f(r_2)$ may be modified by a multiplication of a function $\chi(r_{12})$ which depends on the distance between the electrons. This function $\chi(r_{12})$ is called the correlation function. Several authors like Hylleraas (1929), Hartree and Ingman (1933), and Roothan (1960) have suggested this type of improved approximation of analytical wave function for helium like atoms.

In the present paper we propose to evaluate the nature of the potential functional function and to calculate the cross section of elastic scattering of electron by helium-like atom in the ground state by taking a wave function as suggested by Hartree and Ingman (1933). They have taken both the electrons in the K shell and they argue that the correlation function should approach a constant value for $r_{12} \to \infty$, expressing the separability of the wave function when the electrons are far apart and the decrease to a finite though smaller value for $r_{12} \to 0$. The success of such a wave function can also be judged by the improvement in the value of the eigen-energy. The upper limit for the ground state energy of the helium atom obtained by Hartree and Ingman

using the above wave function is $-2.89e^2/a_0$, a_0 being the Bohr radius, the experimental value being $-2.904e^2/a_0$, whereas Hylleraas, using a wave function without $\chi(r_{12})$, has obtained $-2.847e^2/a_0$ as the value for the same.

In the first part of this paper the function due to Hartree and Ingman has been normalized and the potential function has been evaluated by using the above mentioned wave function. In the second part the differential scattering cross section of electron has been calculated by the Born approximation method neglecting the exchange effect. At 500 eV (the range of energy where the Born approximation method is fairly valid) the differential cross section of scattering of electron by helium atom agrees very well at small angles with the experimental findings of Hughes, McMillen and Webb (1932), but for large angles our theoretical results deviate slightly from the experimental ones. By comparing our results at 700 eV with those of Sachl (1958) who has calculated the same problem in higher Born approximation we find that in the angular range 60° to 135°, our expression gives better agreement with experimental findings than that of Sachl (1958). No data below 60° angle has been given by Sachl.

METHODS OF CALCULATION

The wave function ψ due to Hartree and Ingman is

$$\psi \sim e^{-\xi(r_1+r_2)}(1-Ce^{-\eta r_{12}})$$

where $\xi = 1.8395, \quad C = 0.88784, \quad \eta = 0.047827,$

and the distances are represented in Bohr unit.

The wave function is normalized as shown in Appendix 1.

The potential function is calculated by the formula (vide Mott and Massey, 1949).

$$V(r) = -e^2 \int \left(\frac{Z}{r} - \sum_{n=1,2} \frac{1}{|\boldsymbol{r}-\boldsymbol{r}_n|} \right) |\psi(\boldsymbol{r}_1, \boldsymbol{r}_2)|^2 \, d\boldsymbol{r}_1 \, d\boldsymbol{r}_2, \qquad \ldots (1)$$

where Z is the atomic number and ψ is the wave function.

Thus

$$V(r) = -\frac{Ze^2}{r} + \frac{2e^2}{N^2} \{I(2\xi, 0) - 2CI(2\xi, \eta) + C^2 I(2\xi, 2\eta)\} \qquad \ldots (2)$$

where N is the normalization factor (vide Appendix 1) and

$$I(\mu, \eta) = \int \frac{e^{-\mu(r_1+r_2)-\eta r_{12}}}{|\boldsymbol{r}-\boldsymbol{r}_1|} \, d^3\boldsymbol{r}_1 d^3\boldsymbol{r}_2.$$

From the identity

$$\frac{e^{-\lambda r}}{r} = \frac{1}{2\pi^2} \int \frac{e^{\pm i\boldsymbol{p}\cdot\boldsymbol{r}}}{p^2+\lambda^2} \, d^3\boldsymbol{p}$$

we get

$$I(\mu,\eta) = \frac{\mu^2\eta}{2\pi^8}\int \frac{e^{-i\mathbf{p}.\mathbf{r}_1+i\mathbf{q}.\mathbf{r}_2+i\mathbf{s}.(\mathbf{r}_1-\mathbf{r}_2)-i\mathbf{k}.(\mathbf{r}-\mathbf{r}_1)}}{(p^2+\mu^2)^2(q^2+\mu^2)^2(s^2+k^2)}\, d^3\boldsymbol{r}_1 . d^3\boldsymbol{r}_2 . d^3\boldsymbol{p}\, d^3\boldsymbol{q} . d^3\boldsymbol{s} . d^3\boldsymbol{k}$$

Applying the properties of δ-function

$$\int_{-\infty}^{\infty} e^{\,i(\mathbf{p}-\mathbf{k}).\mathbf{x}}\, d^3\boldsymbol{x} = (2\pi)^3\,\delta(\boldsymbol{p}-\boldsymbol{k})$$

we get

$$\therefore \qquad I(\mu,\eta) = \frac{\mu^2\eta\, 2^5}{\pi^2}\int e^{\,-i\mathbf{k}.\mathbf{r}}\, d^3\boldsymbol{k}\,.\, f(k^2)$$

where

$$f(k^2) = \int \frac{d^3\boldsymbol{s}}{\{(s+k)^2+\mu^2\}^2(s^2+\mu^2)^2(s^2+\eta^2)^2\,.\,k^2}$$

i.e. $$I(\mu,\eta) = \frac{\mu\,\eta\,2^6\pi}{r}\int \frac{1}{ik}\, e^{ikr}\left[\frac{1}{(\mu^2-\eta^2)^2}\left\{\frac{\mu+\eta}{\eta(k^2+\delta^2)(k^2+\lambda^2)} - \frac{4\mu(\mu+\eta)}{(k^2+\delta^2)^2(k^2+\lambda^2)}\right.\right.$$

$$\left.\left. + \frac{2}{(k^2+4\mu^2)^2}\right\} - \frac{2}{(\mu^2-\eta^2)^3}\left\{\frac{1}{(k^2+\delta^2)} - \frac{1}{(k^2+4\mu^2)}\right\}\right] dk$$

where $$\mu+\eta = \delta; \quad \mu-\eta = \lambda$$

After evaluation of the integral we have

$$I(\mu,\eta) = -\frac{2^6\mu\eta\pi^2}{r(\mu^2-\eta^2)^2}\left\{\frac{\mu+\eta}{\eta(\delta^2-\lambda^2)}\left[\frac{1}{\lambda^2} - \frac{e^{-\lambda r}}{\lambda^2} - \frac{1}{\delta^2} + \frac{e^{-\delta r}}{\delta^2}\right]\right.$$

$$-4\mu(\mu+\eta)\left[\frac{1}{\delta^4\lambda^2} - \frac{e^{-\lambda r}}{\lambda^2(\delta^2-\lambda^2)^2} + \frac{e^{-\delta r}}{\delta^2(\delta^2-\lambda^2)^2} + \frac{e^{-\delta r}}{\delta^4(\delta^2-\lambda^2)} + \frac{e^{-\delta r}r}{2\delta^3(\delta^2-\lambda^2)}\right]$$

$$\left. + \frac{1}{8\mu^3}\left[\frac{1}{\mu} - \frac{e^{-2\mu r}}{\mu} - e^{-2\mu r}r\right] - \frac{2}{\delta^2(\mu^2-\eta^2)}[1-e^{-\delta r}] + \frac{[1-e^{-2\mu r}]}{2\mu^2(\mu^2-\eta^2)}\right\}$$

The scattering amplitude, by the Born approximation method is given by

$$f(\theta) = \frac{1}{4\pi}\,\frac{2m}{\hbar^2}\int V(r) e^{\,i\mathbf{k}.\mathbf{r}}\, d^3\boldsymbol{r} \qquad \ldots \quad (3)$$

where $V(r)$ is the potential and $\boldsymbol{k} = \frac{2mv}{\hbar}(\boldsymbol{n}_0-\boldsymbol{n})$, $\boldsymbol{n}_0$ and $\boldsymbol{n}$ are the unit vectors

along the incident and scattered directions respectively. Substituting in Eq. (3) the value of $V(r)$ from Eq. (1) we have,

$$f(\theta) = \frac{e^2}{4\pi}\frac{2m}{\hbar^2}\left[-\int \frac{Z}{r} e^{i\mathbf{k}.\mathbf{r}} d^3\mathbf{r} + \frac{2}{N^2}\{I'(2\xi, 0) - 2CI'(2\xi,\eta) + C^2 I'(2\xi, 2\eta)\}\right] \quad (4)$$

where $$I'(\mu, \nu) = \int_0^\infty \frac{e^{-\mu(\mathbf{r}_1+\mathbf{r}_2)-\nu\mathbf{r}_{12}+i\mathbf{k}.\mathbf{r}}\, d^3\mathbf{r}_1\, d^3\mathbf{r}_2 d^3\mathbf{r}}{|\mathbf{r}-\mathbf{r}_n|}$$

with $$n = 1, 2$$

After integration (vide Appendix 2), we obtain

$$I'(\mu,\nu) = \frac{2^8\pi^3\mu\nu}{k^2}\left[\frac{1}{(\mu^2-\nu^2)^2}\left\{\frac{\lambda/\nu+2}{(k^2+\delta^2)(k^2+\lambda^2)} - \frac{4\mu\delta}{(k^2+\delta^2)^2(k^2+\lambda^2)}\right.\right.$$

$$\left.\left. + \frac{2}{(k^2+4\mu^2)^2}\right\} - \frac{2}{(\mu^2-\nu^2)^3}\left\{\frac{1}{k^2+\delta^2} - \frac{1}{k^2+4\mu^2}\right\}\right]$$

where $$\mu+\nu = \delta, \qquad \mu-\nu = \lambda$$

TABLE I

Comparison of the differential scattering cross section of electron of energy 500 eV scattered by helium atom

Angle in degrees	Differential cross section in units of 10^{-20}cm^2	
	Experimental value	Theoretical results (present author)
9.5	1195.0	1190.4
12.0	1047.0	1037.16
22.0	467.0	475.64
27.0	284.5	287.01
47.0	60.8	69.8
67.0	15.88	20.04
87.0	6.14	9.23

TABLE II

Comparison of the differential scattering cross section of electron of energy 700eV scattered by helium atom

Angle in degrees	Differential cross section in units of 10^{-20} cm^2		
	Experimental value	Theoretical results Sachl	Theoretical results (present author)
60	15	24	15.75
90	5	8.6	4.04
120	3.5	5.2	1.864
135	3.4	1.8	1.405

DISCUSSION

From the calculation it is observed that the screening effect is more prominent far small angles of scattering whereas for large angles it becomes negligible. This is because when the scattering angle is large the particle moves very near the nucleus, where the screening effect due to the surrounding electrons is negligible.

The better agreement of our theoretical calculations with experiment for small angles of scattering is due to the fact that in these cases the particle passes far from the nucleus, where the potential is very weak on account of the screening effect and as such, the perturbation calculations are quite valid.

ACKNOWLEDGMENT

The author is greatly indebted to Prof. D. Basu for suggesting the problem and for his helpful guidance throughout the progress of the work. Thanks are also due to Dr. N. C. Sil for valuable discussion.

APPENDIX I

In the present case the wave function is

$$\psi = \frac{1}{N} e^{-\xi(r_1+r_2)} (1-Ce^{-\eta r_{12}}),$$

the normalization factor N is evaluated from the requirement

$$\int \psi\psi^* d\tau = 1.$$

Thus, $$N^2 = I''(2\xi, 0) - 2CI''(2\xi, \eta) + C^2 I''(2\xi, 2\eta)$$

where $$I''(\mu,\lambda) = \int e^{-\mu(r_1+r_2)}\ e^{-\lambda r_{12}}\ d^3r_1\, d^3r_2$$

$$= 2\pi^2 \int_0^\infty ds \int_0^s du \int_0^u dt\, e^{-\mu s}\ e^{-\lambda u}\ u(s^2-t^2)$$

where $s = r_1+r_2,\quad t = -r_1+r_2,\ u = r_{12}$ (vide Hylleraas, 1929)

$$= 2\pi^2 \int_0^\infty ds \int_0^s du\ e^{-\mu s} e^{-\lambda u}\left(s^2u^2 - \frac{u^4}{3}\right)$$

$$= 2\pi^2 \int_0^\infty ds\ e^{-\mu s}\,(s^2 I_2 - \tfrac{1}{3} I_4)$$

where $I_n = \int_0^s e^{-\lambda u}\ u^n du = \left(-\frac{\partial}{\partial\lambda}\right)^n I_0\ ;\ I_0 = \int_0^s e^{-\lambda u}\, du = \left[\frac{e^{-\lambda u}}{-\lambda}\right]_0^s$

$$\therefore\ I''(\mu,\lambda) = \Big[\int_0^\infty e^{-\mu s}\, s^2 \frac{2}{\lambda^3} ds - \int_0^\infty \tfrac{1}{3} e^{-\mu s}\, \frac{24}{\lambda^5} ds$$

$$- \int_0^\infty e^{-(\lambda+\mu)s} \left\{ \frac{2}{\lambda^3} s^2 + \frac{2}{\lambda^2} s^3 + \frac{1}{\lambda}\ s^4 \right\} ds$$

$$+ \tfrac{1}{3} \int_0^\infty e^{-(\lambda+\mu)s} \left\{ \frac{24}{\lambda^5} + \frac{24}{\lambda^4} s + \frac{12}{\lambda^3} s^2 + \frac{4}{\lambda^2} s^3 + \frac{1}{\lambda} s^5 \right\} ds\ \Big]$$

i.e., $$I''(\mu,\lambda) = \frac{8\pi^2}{\mu^3(\lambda+\mu)^5}\ \{\lambda^2+5\lambda\mu+8\mu^2\}$$

Since $$\int_0^\infty e^{-\nu s}\ s^n\, ds = \frac{n!}{\nu^{n+1}}$$

APPENDIX 2

The value of $I'(\mu,\nu)$ we get as

$$I'(\mu,\nu) = \int\int\int \frac{e^{\ -\mu(r_1+r_2)-\nu r_{12}+i\mathbf{k}\cdot\mathbf{r}}\ d^3\mathbf{r}_1\, d^3\mathbf{r}_2\, d^3\mathbf{r}_3}{|\mathbf{r}-\mathbf{r}_1|}$$

$$= \frac{\mu^2\nu}{(\pi^2)^3 2\pi^2} \int\int\int \frac{e^{-i\mathbf{p}.\mathbf{q}(\mathbf{r}-\mathbf{r}_1)}}{p^2}\, d^3\boldsymbol{p} \int \frac{e^{i\mathbf{q}.\mathbf{r}}}{(q^2+\mu^2)^2}\, d^3\boldsymbol{q} \int \frac{e^{i\mathbf{t}.\mathbf{r}_2}}{(t^2+\mu^2)^2}\, d^3\boldsymbol{t}$$

$$\int \frac{e^{i\mathbf{s}.(\mathbf{r}_1-\mathbf{r}_2)}}{(s^2+\nu^2)^2}\, d^3\boldsymbol{s} \int e^{i\mathbf{k}.\mathbf{r}} d^3\boldsymbol{r}\, d^3\boldsymbol{r}_1\, d^3\boldsymbol{r}_2$$

Since
$$\frac{e^{-\lambda r}}{r} = \frac{1}{2\pi^2} \int_{-\infty}^{\infty} \frac{e^{i\mathbf{p}.\mathbf{r}}}{p^2+\lambda^2}\, d^3\boldsymbol{p}$$

and
$$e^{-\lambda r} = \int_{-\infty}^{\infty} \frac{e^{i\mathbf{p}.\mathbf{r}} d^3\boldsymbol{p}}{(p^2+\lambda^2)^2}$$

$$\therefore \quad I'(\mu, \nu) = \frac{\mu^2\nu(2\pi)^9}{2\pi^8} \int \frac{\delta(\boldsymbol{k}-\boldsymbol{p})\delta(\boldsymbol{p}+\boldsymbol{q}+\boldsymbol{s})\delta(\boldsymbol{t}-\boldsymbol{s}) d^3\boldsymbol{p}\, d^3\boldsymbol{q}\, d^3\boldsymbol{t}\, d^3\boldsymbol{s}}{p^2(q^2+\mu^2)^2(t^2+\mu^2)^2(s^2+\nu^2)^2}$$

$$= \frac{2^8\mu^2\nu\pi}{\boldsymbol{k}^2} \int \frac{d^3\boldsymbol{s}}{(|\boldsymbol{k}+\boldsymbol{s}|^2+\mu^2)^2(s^2+\mu^2)^2(s^2+\nu^2)^2}$$

$$= \frac{2^8\pi^2\mu^2\nu}{\boldsymbol{k}^3} \int \frac{\boldsymbol{s}\; d\boldsymbol{s}}{(s^2+\mu^2)^2(s^2+\nu^2)^2\{(s-k)^2+\mu^2\}}$$

Applying the following identity,

$$\left[\, (p^2+\mu^2)(p^2+\nu^2) \,\right]^{-2} = \frac{1}{(\mu^2-\nu^2)^2} \left[\frac{1}{(p^2+\nu^2)^2} + \frac{1}{(p^2+\mu^2)^2} \right]$$

$$- \frac{2}{(\mu^2-\nu^2)^3} \left[\frac{1}{(p^2+\nu^2)} - \frac{1}{(p^2+\mu^2)} \right]$$

$$\therefore\ I'(\mu, \nu) = \frac{2^8\pi^3\mu\nu}{\boldsymbol{k}^2} \left[\frac{1}{(\mu^2-\nu^2)^2} \left\{ \frac{1}{(\boldsymbol{k}^2+\delta^2)(\boldsymbol{k}^2+\lambda^2)} \left\{ \frac{\mu-\nu}{\nu} + 2 \right] - \frac{4\mu(\mu+\nu)}{(\boldsymbol{k}^2+\delta^2)^2(\boldsymbol{k}^2+\lambda^2)} \right.\right.$$

$$\left.\left. + \frac{2}{(\boldsymbol{k}^2+4\mu^2)^2} \right\} - \frac{2}{(\mu^2-\nu^2)^3} \left\{ \frac{1}{\boldsymbol{k}^2+\delta^2} - \frac{1}{\boldsymbol{k}^2+4\mu^2} \right\} \right]$$

where
$$\mu+\nu = \delta \quad \text{and} \quad \mu-\nu = \lambda$$

REFERENCES

Hartree D. R., and Ingman, 1933, *Mem. Proc. Manchester. Lit & Phil Soc.* **77**, 79.
Hughes, A. L., McMillen, J. H. and Webb, G. M. 1932, *Phys. Rev.* **58**, 154.
Huzinaga, S., 1960, *Prog. Theo. Phys.*, **23**, 562.
Hylleraas, E. A., 1929, *Z. Physik.*, **54**, 347.
Mott, N. F. & Massey, H. S. W. 1949, Theory of Atomic Collision, Oxford University Press, New York. (2nd Edition).
Roothan, C. C. J., 1960, *Rev. Mod. Phys.*, **32**, 178, 194.
Sachl, V., 1958, *Phys. Rev.*, **110**, 891.

DETERMINATION OF PHOTOELASTIC CONSTANTS IN THE PRESENCE OF TILT OF THE AXES

K. V. KRISHNA RAO

Physics Department, Osmania University, Hyderabad-7

(*Received January* 2, 1961)

ABSTRACT. This paper describes a direct method of determining the differential stress-optical constants, when the axes of polarisation in a stressed crystal do not coincide with the principal directions of stress. The method is verified by studies on barium nitrate and strontium nitrate crystals.

INTRODUCTION

With the application of the group-theoretical methods by Bhagavantam (1942) to derive the number of non-vanishing photoelastic constants for different classes of crystals and the discovery of several errors in the schemes given earlier by Pockels (1889), interest in the photoelastic effect in crystals was revived and an intensive study of the subject was undertakn by Bhagavantam and collaborators in recent years (Nye, 1957; Krishnan, 1958). During the course of these studies, it was found (Bhagavantam and Krishna Rao, 1953a) that, for some orientations of cubic crystals, the principal axes of polarisation of the stressed crystal do not coincide with the principal directions of stress. This phenomenon has been referred to as the tilt of the axes. When there is tilt of the axes, if the usual experimental method for determining the differential stress-optical constants, is employed, one should first find the positions of the axes of polarisation of the stressed crystal and adjust the Babinet compensator, such that its principal directions coincide with the axes of polarisation of the stressed crystal. On the other hand, if the principal directions of the compensator are kept vertical and horizontal, as usual, and the crystal is stressed vertically, it has been found that the shift of the Baninet fringe is not proportional to the applied stress and the fringe vibrates about the initial position, as the stress is gradually increased. It will now be shown that, from a knowledge of the stress required to bring back the Babinet fringe to its initial position, the stress-optional constant can be evaluated directly, without necessitating the determination of the tilt of the axes.

THEORY

Let OX_1, OY_1 (Fig. 1) be the principal directions of polarisation of the stressed crystal in the XY plane (normal to the direction of observation), OX_2, OY_2 the

principal directions of the compensator and OP the direction of vibration of the incident plane polarised beam of light of amplitude a. Let α and β be angles X_1OP and X_1OX_2 respectively.

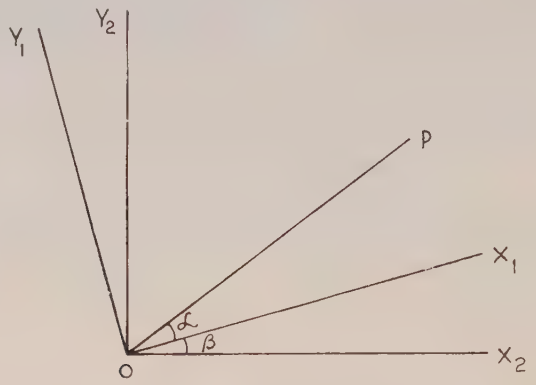

Fig. 1. Showing the principal directions of the stressed crystal (OX_1, OY_1), the principal directions of the compensator (OX_2, OY_2) and the direction of vabration (OP) of the incident light.

On entering the stressed crystal, the incident beam will be resolved into two components, one of amplitude $a \cos \alpha$ and direction of vibration OX_1 and the other of amplitude $a \sin \alpha$ and direction of vibration OY_1. These components will have a phase difference, say δ, when they leave the crystal. When the beam enters the compensator, each of the above-mentioned two components will split further into two components with their vibration directions along OX_2 and OY_2. The amplitude of the component, with the vibration direction along OX_2, is the resultant of the two components of amplitudes $a \cos \alpha \cos \beta$ and $-a \sin \alpha \sin \beta$ and phase difference δ. Similarly, the amplitude of the component with vibration direction along OY_2 is the resultant of two components of amplitudes $a \sin \alpha \cos \beta$ and $a \cos \alpha \sin \beta$ and phase difference δ. The amplitude A of the component with the vibration direction along OX_2 is given by

$$A^2 = a^2\{\cos^2(\alpha-\beta)-\tfrac{1}{2} \sin 2\alpha \sin 2\beta(1+\cos \delta)\}. \quad \ldots (1)$$

The phase of this vibration Δ_1 is given by

$$\tan \Delta_1 = -\frac{\sin \alpha \sin \beta \sin \delta}{\cos \alpha \cos \beta - \sin \alpha \sin \beta \cos \delta} \quad \ldots (2)$$

Similarly, the amplitude B of the component whose vibration direction is along OY_2 is given by

$$B^2 = a^2 \{\sin^2 (\alpha+\beta)-\tfrac{1}{2} \sin 2\alpha \sin 2\beta(1- \cos \delta)\} \quad \ldots (3)$$

and its phase Δ_2 is given by

$$\tan \Delta_2 = \frac{\sin \alpha \cos \beta \sin \delta}{\cos \alpha \sin \beta + \sin \alpha \cos \beta \cos \delta} \quad \ldots \quad (4)$$

From Eqs. (2) and (4), we get

$$\tan (\Delta_2 - \Delta_1) = \frac{\sin 2\ \alpha\ \sin \delta}{\sin 2(\alpha+\beta) - 2 \cos 2\beta\ \sin 2\alpha\ .\ \sin^2 \delta/2} \quad \ldots \quad (5)$$

The fringe shift in the compensator gives $(\Delta_2 - \Delta_1)$ which would obviously be equal to δ when the tilt of the axes β is zero. Eq. (5) shows that, as δ is increased, $(\Delta_2 - \Delta_1)$ first increases, reaches a maximum and then reduces to zero when $\delta = \pi$. On a further increase of δ, $\Delta_2 - \Delta_1$ changes sign, reaches a maximum and again reduces to zero when $\delta = 2\pi$. Thus the Babinet fringe completes one oscillation as the phase difference δ increases from zero to 2π. The variation of $\Delta_2 - \Delta_1$ with δ, evaluated for values of α and $(\alpha+\beta)$, 30° and 45° respectively, using Eq. (5), is shown in Fig. 2. It is clear that the strees P, required for one complete

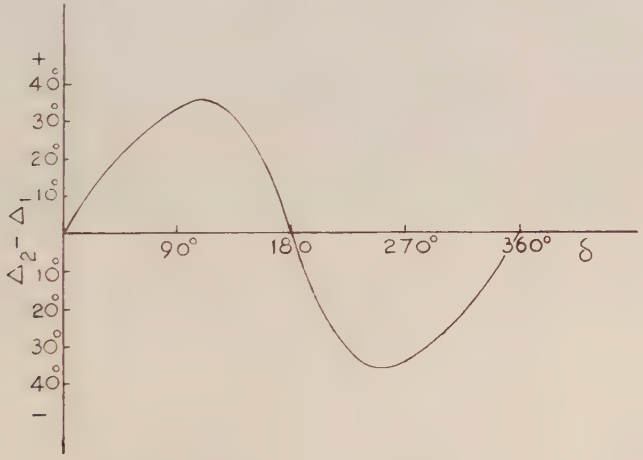

Fig. 2. Variation of $(\Delta_2 - \Delta_1)$ with δ.

oscillation of the Babinet fringe, gives the stress required for a path difference λ (wavelength of the light used) between the two components with their vibration directions along the principal directions of the stressed crystal. Hence the differential stress-optical coefficient C is given by

$$C = \frac{2\lambda}{n^3 P t},$$

where t is the thickness of the crystal parallel to the direction of observation and n the refractive index of the crystal in the unstressed state.

EXPERIMENTAL

To verify the foregoing method, crystal prisms of barium nitrate and strontium nitrate, with faces parallel to (111), $(01\bar{1})$ and $(\bar{2}11)$ planes, have been studied applying the stress, by a lever arrangement, along $[\bar{2}11]$ and making the observations along $[01\bar{1}]$ employing the usual arrangement (Fig. 3) for determining the differential stress-optical constants. The stress-optical constant C for this ori-

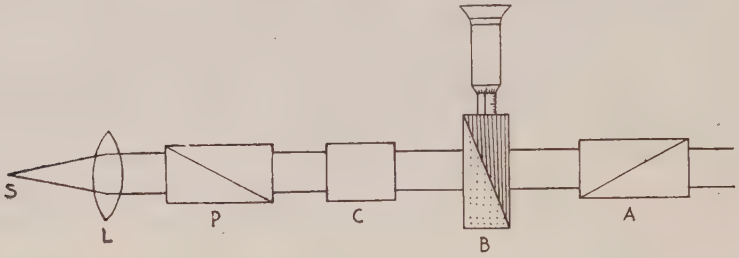

Fig. 3. Experimental set-up for determining differential stress-optical constants.
S—Source of light
L—Condensing lens
P—Polarising Nicol
C—Crystal
B—Babinet compensator
A—Analysing Nicol

entation of T_h (m_3) class of crystals, to which these two substances belong, is related to the stress-optical coefficients q_{11}, q_{12}, q_{13} and q_{44} by (Bhagavantam, 1953) :

$$C = \tfrac{1}{3}\sqrt{\tfrac{1}{4}\ (A+5q_{44})^2+2(A-q_{44})^2} \qquad \ldots \quad (7)$$

where, $\qquad A = \tfrac{1}{2}\,(2q_{11}-q_{12}-q_{13})$.

In the case of barium nitrate, the load required for one oscillation of the Babinet fringe is found to be 2380 grams, the mechanical advantage of the lever arrangement being 3.992. The length of the prism parallel to [111] direction, which enters the calculations, is 0.330 cm. With these values, taking n as 1.570 (Landolt and Bornstein, 1931), the stress-optical constant is evaluated, using Eq (6). The value obtained, 10.8×10^{-13} cm^2 dyne^{-1}, is found to be in agreement with 10.2, evaluated using Eq. (7), taking the values of A and q_{44} (Bhagavantam and Krishna Rao, 1953b) as 20.60 and 1.69 respectively.

For strontium nitrate, the load for one oscillation of the Babinet fringe is 3300 grams. The length of the prism parallel to [111] is 0.264 cm. The stress-optical constant, evaluated using Eq. (6), taking n as 1.567 (Landolt and Bornstein, 1931) is found to be 6.3, in close agreement with 6.27, evaluated using Eq (7),

taking A and q_{44} ((Bhagavantam and Krishna Rao, 1954) as 13.61 and 1.38 respectively.

REFERENCES

Bhagavantam, S., 1942, *Proc. Ind. Acad. Sci.*, **A16**, 359.
Bhagavantam, S., 1953, *Proc. Ind. Acad. Sci.*, **A37**, 585.
Bhagavantam, S., and Krishna Rao, K. V., 1953a, *Proc. Ind. Acad. Sci.*, **A37**, 589.
Bhagavantam, S., and Krishana Rao, K. V., 1953b, *Acta Cryst.*, **6**, 799.
Bhagavantam, S., and Krishna Rao, K. V., 1954, *Curr. Sci.*, **23**, 257.
Krishnan, R. S., 1958, Progress in Crystal Physics, Madras.
Landolt, H. H. and Bornstein, R., 1931, Physikalische Chemische Tabellen.
Nye, J. F., 1957, Physical Properties of Crystals, Oxford : Clarendon Press.
Pockels, F., 1889, *Ann. der. Phys.*, **37**, 144.

39

STUDY OF ULTRASONIC VELOCITY IN LIQUIDS

P. R. K. L. PADMINI AND B. RAMACHANDRA RAO

ULTRASONIC LABORATORY, PHYSICS DEPARTMENT, ANDHRA UNIVERSITY, WALTAIR

(*Received January* 11, 1961)

ABSTRACT. Ultrasonic velocity measurements are carried out in a number of new organic liquids, low melting point organic solids in the molten state and corrosive inorganic liquids. The important constants adiabatic compressibility, β_{ad}, γ, C_v, Van der Waals' "b" and molecular radii are computed. A method different from that of Schaaffs was followed in computing the value of "b" for atoms and linkages and the values for some atoms and linkages are obtained. It is found that the contribution of semipolar bond to Van der Waals' "b" is negative.

INTRODUCTION

Extensive studies of ultrasonic velocity in liquids and their interpretation in the light of molecular structure have been made by several investigators like Parthasarathy (1935, 1936, 1937), Schaaffs (1945, 1950, 1951), Baccaredda and Giacomini (1945, 1946, 1947, 1949, 1950), Lagemann (1948, 1953, 1957), Rao and others (1940, 1941). An important advance has been made when Rao (1941) has discovered R the molar sound velocity, a temperature independent constant and it is characteristic of the atoms and linkages in a molecule. Schaaffs (1957) has shown that the measurement of ultrasonic velocity enables the computation of certain thermodynamic constants such as β_{ad} and C_v and the molecular constants as Van der Waals' "b" and molecular radii. It has already been established by many workers that Van der Waals' "b" is an additive function of the atoms and linkages as some other physical properties like parachor "P" critical volume "Vc" etc. Schaaffs (1950) has given values of b for various elementary groups and atoms with different linkages. He tested the validity of this additive law in some compounds and obtained a good agreement between the calculated and experimental values of "b" as well as ultrasonic velocity "V".

In the present investigation the authors presented the ultrasonic velocity data and the various thermodynamic constants for many new liquids. An attempt is made to compute the value of Van der Waals' "b" for atoms and various linkages by following a method different from that of Schaaffs and it is tested in many common organic liquids for which the ultrasonic velocity data are available.

RESULTS

The ultrasonic velocity data along with the various constants calculated for the liquids studied are presented in Table I. The ultrasonic velocities for the

TABLE I

Compound	Temp °C	Velocity m/s V	β_{ad} X 10 cm²/ dyne	Ratio of specific heat	C_v	rX10⁸ cm	r from
Diethylamine	23.5	1103	118.00	1.149	1.8870	2.142	2.133 (27.5°C)
Isopropylamine	20.0	1089	123.50	—	—	1.994	1.998 (27.5°C)
Dimethyl sulphate	31.0	1223	50.74	—	—	2.075	2.018 (27.0°C)
Diethyl sulphate	31.2	1199	59.17	—	—	2.310	2.320
Sulphur chloride	26.0	1173	43.57	2.187	0.4211	1.956	2.272 (20.8°C)
Thionyl chloride	30.6	1023	58.86	2.197	0.4610	1.894	2.061 (10.0°C)
Sulphuryl chloride	30.6	925	70.50	1.877	0.5194	1.961	2.041 (20.0°C)
Triethyl phosphate	30.6	1226	62.59	—	—	2.513	2.811 (27.5°C)
Triphenyl phosphate	58.0	1385	43.33	—	—	2.961	3.239 (55.0°C)
Azoxy benzene	29.9	1532	36.43	—	—	2.530	2.922 (27.5°C)
Azo benzene	67.7	1355	52.29	1.299	1.0620	2.538	—
Vinyl acetate	25.7	1122	85.88	—	—	1.783	1.809 (27.0°C)
Methyl methacrylate	29.7	1179	76.58	—	—	2.140	2.186
Ethyl methacrylate	25.0	1180	78.57	—	—	2.258	2.309
Naphthalene	89.6	1183	73.07	1.317	0.3045	2.294	2.403 (99.0°C)
Diphenyl	74.8	1361	54.69	—	—	2.466	2.746 (78.0°C)
Phenyl salicylate	69.8	1336	48.34	1.232	1.3280	2.592	2.885 (48.0°C)
Maleic anhydride	86.2	1433	35.91	—	—	1.893	—
Phenol	64.6	1396	49.49	1.237	1.8920	2.354	2.220 (45.0°C)
p-dichloro benzene	67.7	1118	64.83	1.487	0.8390	2.227	2.437 (56.0°C)
Antimony trichloride	100.0	88.8	38.59	—	—	1.997	—
Sodium acetate	90.0	1701	27.10	—	—	—	—

TABLE II

Temperature 20°C

Compound	Formula	Experimental value of "b"	Computed value of "b"
Nonane	C_9H_{20}	164.60	161.70
Ethyl alcohol	C_2H_5OH	52.46	52.08
Propyl alcohol	C_3H_7OH	64.62	67.51
Pentachloro ethane	$C_2H_5Cl_5$	127.20	122.00
Tetrachloro ethane	$C_2H_2Cl_4$	99.65	106.20
Carbon tetrachloride	CCl_4	90.63	90.79
Amyl bromide	$C_5H_{11}Br$	116.10	108.20
Bromoform	$CHBr_3$	83.03	84.08
Tetrabromo ethane	$C_2H_2Br_4$	111.90	118.50
Propyl iodide	C_3H_7I	91.52	88.77
Ethyl iodide	C_2H_5I	75.08	73.34
Chloro benzene	C_6H_5Cl	96.23	95.67
Orthochloro toluene	$C_6H_5CH_2Cl$	122.80	111.10
Toluene	$C_6H_5CH_3$	100.30	95.38

Table III

Values of Van der Waals' 'b' for some atoms and linkages

C = 3.23	
H = 6.11	
N = 16.14	
Cl = 21.89	(=) in (C=0) = 12.55
Br = 24.95	(=) i (C=C) = 24.05
I = 36.38	(=) = 8.11
S = 17.50	Benzene ring = 23.90
P = 15.95	
Sb = 12.71	
0 = 9.02	

TABLE IV

Temperature 20°C

	Compound	Velocity (m/sec) V	Density (gm/cc)	Experimental value of "b"	Computed value of "b"
*	Diethylamine	1150	0.7071	96.16	96.16
	Isopropylamine	1089	0.6836	79.69	81.73
*	Dimethyl sulphate	1255	1.333	89.82	89.82
	Diethyl sulphate	1244	1.188	123.30	121.38
*	Sulphur chloride	1198	1.622	78.79	78.79
	Thionyl chloride	1148	1.839	60.94	65.59
	Sulphuryl chloride	940	1.673	75.48	75.91
	Ethyl phosphate	1219	1.074	152.40	158.90
	Triphenyl phosphate	1510	1.236	184.90	269.30
	Azo benzene	1494	1.083	161.70	203.90
	Azoxy benzene	1558	1.180	161.90	208.90
	Vinyl acetate.	1152	0.9315	96.36	104.16
	Methyl methacrylate	1220	0.949	99.19	119.59
	Ethyl methacrylate	1201.5	0.919	117.00	134.80
	Naphthalene.	1392	1.030	118.50	132.80
	Diphenyl	1534	1.035	149.00	147.60
	Phenyl salicylate	1489	1.196	172.50	190.40
	Phenol	1528	1.079	82.77	88.90
	p-dichloro benzene	1252	1.292	108.10	110.50
*	Antimony trichloride.	1128	2.780	78.38	78.38
*	Phosphorus trichloride	995	1.580	81.62	81.62

*These liquids have been taken for standardization.

organic liquids and the low melting point organic solids are measured by the fixed path variable frequency interferometer. The corrosive liquids are studied with a special type of all glass cell using pulse techniques. The glass cell is made by fusing two parallel ground glass plates to the two ends of a cylindrical tube. The length of the cell is about 4.5 cms. The crystals are attached to the two sides of the cell. The liquids used are of E. Merck samples. The densities are determined by a specific gravity bottle. The physical constants, specific heat and thermal expansion required in computing the constants C_V, γ are taken from

International Critical Tables. As the measurements reported in Table I are made at different temperatures, the ultrasonic velocities in all the different substances are reduced to the same temperature of 20°C to facilitate comparison by using the known temperature variation data obtained by the authors. The results thus obtained are presented in Table IV along with Van der Waals' "b" and density.

It may be noticed that there are some low melting point solids in which the ultrasonic velocity is measured in the liquid state at temperature above the melting point. The values of ultrasonic velocity given for these substances extrapolated to 20°C represent hypothetical values which these substances would have had if they exist in liquid state at 20°C.

DISCUSSION

The velocity data represented in Table IV follows well the rules proposed by Parthasarathy (1935, 1936, 1937) and Schaaffs (1948). After a detailed study of the ultrasonic velocity data available in the liquid state the authors also arrived at the general conclusion that in the homologous or progressive series of organic molecules the ultrasonic velocity varies in the same sense as the density, i.e., increasing with increase in density or decreasing with decrease in density progressively for higher members. The compressibility variation is exactly opposite. Exceptions to this rule are found in the series involving either a halogen atom or a lighter group (COOH, CH_3, etc).

Examining the velocity data in the light of the rules proposed by Parthasarathy (1937), Schaaffs (1950) and by the authors it is seen that the velocity is higher and the compressibility is lower in diethylamine than that in isopropylamine which has less chain length. Ultrasonic velocities in the monomers, methyl methacrylate and ethyl methacrylate also show a decrease for the higher member along with a decrease in density and this feature is also similar and in agreement with the general rule. The compounds ethyl sulphate and methyl sulphte also follow the same rule, though the acid radical is inorganic.

The interesting result which the authors obtained from a study of the sulphur compounds, $SOCl_2$, SO_2Cl_2 is that the presence of a semipolar double bond reduces the ultrasonic velocity. This is confirmed when we remember the fact that the contribution of semipolar double bond to molar sound velocity is negative. The high velocities of maleic anhydride and phenol may be attributed to the presence of hydroxyl groups which enhance the velocity according to Parthasarathy (1937). Comparison of measurements for the two phosphates involves an aliphatic and an aromatic compound. The triphenyl phosphate has a high molecular weight and higher density than triethyl phosphate. Besides it has the contribution of three benezene rings whose presence always increases the velocity; on both these considerations the ultrasonic velocity in triphenyl phosphate is higher than that in triethyl phosphate. A study of the structures of the two compounds azobenzene

and azoxybenzene reveals that the azoxybenzene contains one additional oxygen atom besides a semipolar bond. It is known that the effect of addition of an atom or an increase of molecular weight is generally to increase the velocity while the semipolar bond has the effect of decreasing the velocity. As the ultrasonic velocity increases for the latter accompanied by an increase of density it appears that the increase of velocity due to addition of oxygen atom is greater than the negative effect of the semipolar bond. Again the parallel increase of density and velocity and the decrease of compressibility for the higher member is in accordance with the general rule of velocity variation with density given by the author.

Comparing the velocities of naphthalene, diphenyl and phenyl salicylate, the diphenyl is a longer molecule with high molecular weight and density than naphthalene and this again leads to further increase in velocity and decrease in compressibility. Phenyl salicylate shows a departure from this behaviour and it has not been possible to explain this variation.

Phenol and paradichlorobenzene are substitution compounds of benzene and it will be appropriate to compare the velocities of the three substances at 20°C. The velocity of phenol is greater than that in benzene due to the presence of the hydroxyl group and the velocity of *p*-dichlorobenzene is less than that in benzene due to the presence of two chlorine atoms.

It is well known that the ratio of specific heats generally lies between 1 and 1.5 for all the organic liquids. In the present investigation the range of the values computed for some liquids which lie between 1.237 and 1.482 is the agreement with the general range of variation expected for organic liquids. In the case of the few inorganic liquids, the γ values are quite high being greater than 1.8. The C_V and γ values for some of the liquids investigated are obtained for the first time and are reported in Table I. Schaaffs (1951) has shown that Van der Waals' "b", and the molecular radii r of any molecule can be calculated from the relations.

$$b = \frac{M}{\rho}\left[1 - \frac{RT}{MV^2}\left\{\sqrt{\frac{1+MV^2}{3RT}} - 1\right\}\right]$$

$$r = \sqrt[3]{\frac{3b}{16\pi N}}$$

where M = Molecular weight
ρ = density
T = Temperature in degrees absolute
V = Velocity of sound
R = Gas constant

b = Van der Waals' b
N = Avogadro number

r can also be calculated from the refractive index measurements by using the relation.

$$r = 3\sqrt{\frac{3}{4\pi N}\,\frac{\mu^2-1}{\mu^2+2}\,\frac{M}{\rho}}$$

where μ = refractive index

The r values calculated by both these methods for most of the liquids investigated are presented in Table I. It will be seen that these values obtained by both these methods are in good agreement with each other. Although there are significant deviations in the case of the inorganic compounds like sulphur chloride, thionyl chloride and triphenyl phosphate, and also in azoxy benzene this discrepancy may be attributed partly to structural influences and partly to the impurity of chemicals.

From a study of the ultrasonic velocities in homologous series of organic liquids at 20°C Schaaffs has deduced the b values for some of the common elements having certain common linkages as for instance, $-H->C<>C=0=(C)$, etc. He has also calculated b values for certain organic groups which commonly occur in organic liquids. He has given different values for these groups depending on whether they are linked to aliphatic series or aromatic series. As b is found to be additive in nature, Schaaffs (1948) has calculated the b values for several organic liquids using the data for groups and atoms thus obtained, and compared these with the values calculated from ultrasonic velocities and found them to be in good agreement.

The authors have attempted an investigation on similar lines following however, a different procedure for the computation of Van der Waals' b. While Schaaffs has considered "b" values for atoms and atomic groups, the authors have considered the contribution as due to atoms and linkages like double, triple, and semipolar double bonds. The values thus obtained for various atoms linkages and ring structures using the data available in literature for some common organic liquids are given in the Table III. To check up the accuracy in the estimation of b values obtained for atoms and linkages, the b values for some other organic liquids are calculated from the ultrasonic velocity data and are compared with the computed values. This data is presented in Table III. Considering the fact that "b" is constitutive in nature to a certain extent and that the value of b for the same atom linked with different atoms has generally slightly different values, the agreement may be taken as quite satisfactory. Such of those differences which are significant may be attributed to the constitutive influences.

Using the "b" values for atoms, the b value for semipolar double bond is deduced from the calculated b value from ultrasonic velocities of the five liquids,

ethyl phosphate, methyl and ethyl sulphate, thionyl and sulphuryl chlorides, leaving the two liquids azoxy benzene and triphenyl phosphate. The interesting result was that the contribution of Van der Waals' b to semipolar linkage is negative and small. The negative value for b indicates that there is effectively a contraction in the volume of the molecule. This result is analogous to the negative value of parachor reported by Sugden (1930) and of molar sound velocity obtained by us. Since the structural formulae of azoxy benzene and triphenyl phosphate are quite large involving benzene ring and double bonds, the values of b estimated for them are not accurate. Perhaps that may be the reason why the contribution for semipolar bond in the two liquids turned up as positive.

Comparing the experimental values of b with the computed ones for the liquids investigated here, the agreement may be considered as gratifying for most of the liquids except naphthalene, phenyl salicylate, triphenyl phosphate, azo and axoxy benzenes. The large deviations observed in these liquids are due to constitutive effects which sometimes alter the values of the individual atomic contributions widely.

Since Schaaffs (1950) has attributed "b" values for groups instead of linkages it has limited application in computing the b value for a new liquid. According to his method the values for a large number of groups are to be known in order to compute the value of b for any new liquid, since there are so many possible combinations of atoms with various linkages, occurring normally in all the organic liquids. The author's method has wide application in the computation of "b' values for liquids but some times the computed values show large deviations from the experimental results due to consitutive influences.

REFERENCES

Baccaredda, M. and Gaicemini, A., 1945, *Ricera Scientifica*, **15**, 161.
Baccaredda, M. and Gaicemini, A., 1946, *Ricera Scientifica*, **16**, 611, 662.
Baccaredda, M. and Gaicemini, A., 1947, *Ricera Scientifica*, **17**, 1108.
Baccaredda, M. and Gaicemini, A., 1949, *Ricera Scientifica*, **19**, 358.
Baccaredda, M. and Gaicemini, A., 1950 *Ricera Scientifica*, **20**, 133.
Lagemann, R. T., 1948, *J. Chem. Phys.*, **16**, 247.
Lagemann, R. T., 1953, *J. Chem. Phys.*, **21**, 819.
Lagemann, R. T., 1948, *J. Am. Chem. Soc.*, **70**, 2994, 2996,
Lagemann, R. T., 1957, *J. Am. Chem. Soc.*, **73**, 3213, 5891.
Lagemann, R. T. and Dunbar, W. S., 1949, *J. Phys. Scham.*, **49**, 428.
Parthasarathy, S., 1935, *Proc. Ind. Acad. Sci.*, **2**, 497.
Parthasarathy, S., 1936, *Prob. Ind. Acad. Sci.*, **3**, 285, 518.
Parthasarathy, S., 1937, *Proc. Ind. Acad. Sci.*, **4**, 59, 213.
Rao, M. R., 1940, *Ind. J. Phys.*, **14**, 109.
Rao, M. R., 1941, *J. Chem. Phys.*, **9**, 682.
Schaaffs, W., 1948, *Zeits. Natur. for sch.*, **13**A, 396.
Schaaffs, W., 1950, *Zeits. Phys. Chem.*, **195**, 136.
Schaaff's W., 1951. *Zeits. Phys. Chem.*, **196**, 397, 413.
Sugden, S., 1930, Parachor and Valeney.

40

GAS PROPERTIES AT HIGH TEMPERATURES ON THE EXPONENTIAL MODEL

P. K. CHAKRABORTI

Indian Association for the Cultivation of Science, Jadavpur, Calcutta-32

(*Received March* 15, 1961)

ABSTRACT. High temperature viscosity data have been utilised to obtain the potential parameters for the exponential model for He, A, N_2, O_2 and CO_2. These parameters can reproduce the experimental viscosity data at high temperatures more satisfactorily than the parameters determined from scattering experiments. The combination rules proposed for the exponential model have been tested in relation to the high temperature inter-diffusion coefficient and the results so obtained are discussed.

INTRODUCTION

The knowledge of the gas properties at high temperatures is of great importance particularly in connection with high speed gas dynamics, combustion, detonation etc. In the experimental determination of the required gas properties at very high temperatures, many difficulties are to be surmounted and even then the results are liable to large errors. Further, the graphical extrapolation of the low temperature data is likely to give unsatisfactory results at high temperatures. More satisfactory values for the transport coefficients can, however, be obtained by calculating the intermolecular potential from high temperature properties and utilising the equations of the kinetic theory to calculate the required transport property.

At high temperatures small intermolecular separations are predominant (Hirschfelder *et al.*, 1954). Above the Boyle point the attractive part of the intermolecular potential becomes less important than the repulsive part. Hence in the consideration of the high temperature gas properties we may neglect the attractive part of the potential and assume only the repulsive part (Cottrell, 1956). At low and intermediate temperatures the intermolecular potential is believed to be represented reasonably well by the various molecular models (e.g. Lennard-Jones 12 : 6, exp-6, etc.), but their applicability to gases at high temperatures is open to question (1958a, 1958b).

Amdur and his co-workers (1954-57) have tried to fit their molecular scattering data to a potential of the form

$$\phi(r) = \frac{A}{r^s} \qquad \ldots \quad (1)$$

where A and s are constants and r is the intermolecular separation. Subsequently Amdur and Mason (1958a) have calculated a large number of gas properties at high temperatures from the low and intermediate temperature data and have suggested that a potential of the form

$$\phi(r) = A\, e^{-\frac{r}{\rho}} \qquad \ldots \quad (2)$$

may be able to reproduce the experimental data over a wide range of temperatures than the inverse power model. They have obtained the constants A and ρ for several substances from the scattering experiments, but could not test the accuracy of the values by comparison with experimental transport property data, as the collision integrals on the exp-model were not available. Quite recently Monchick (1959) has evaluated the various collision integrals on the exp-model ; therefore evaluation of the potential parameters from transport data is also possible. Walker and Westenberg (1960) have utilised these collision integrals to determine the unlike potential parameters from their experimental diffusion data for the gas pairs CO_2—O_2. CH_4—O_2. H_2O—O_2 and CO—O_2 and obtained some interesting results. In the present paper we have determined the potential parameters for the exponential model from the data on high temperature viscosity of pure components. These have been compared with the values available from other sources.

CALCULATION OF POTENTIAL PARAMETERS FROM HIGH TEMPERATURE VISCOSITY

Large amount of experimental data in the temperature range where Eq. (2) is applicable exists for viscosity (1930, 1945, 1958, 1959). It was, however, found that the constants A and ρ given by Amdur and Mason (1958) fail to reproduce these data satisfactorily. Hence it was felt desirable to obtain the constants A and ρ on the exponential model directly from the viscosity data at high temperatures. These constants are likely to reproduce the transport properties better than those determined from the scattering data. The viscosity data for He, A, N_2, O_2 and CO_2 in the temperature range 800°K—1500°K were utilised for this purpose.

On the Chapman-Enskog theory the viscosity coefficient η is given to the first approximation as (Hirschfelder *et al.*, 1954).

$$[\eta]_1 \times 10^7 = 266.93\sqrt{T} \times M/\sigma^2\Omega^{(2,2)*}\ g/\text{cm-sec.} \qquad \ldots \quad (3)$$

where T is the absolute temperature. M the molecular weight of the substance $\Omega^{(2,2)*}$ are the collision integrals, σ is some arbitrary length parameter which is defined by $\phi(r)$ and is given by (Monchick, 1959).

$$\sigma^2\Omega^{(l,s)*} = 8\alpha^2\rho^2 I_{(l,s)}(\alpha)/(s+1)![1-\tfrac{1}{2}\{1+(-1)^l\}/(1+l)] \qquad \ldots \quad (4)$$

where l, s are integral numbers, $I(\alpha)_{(l,s)}$ are in the form of integrals depending upon α, and α is related to A in Eq. (2) by (Monchick, 1959).

$$\alpha = \ln (A/kT) \qquad \ldots \quad (5)$$

Values of the integrals $I(\alpha)_{(l,s)}$ are tabulated (Monchick, 1959) as function of α.

Comparing Eq. (3) and (4) we get ($l = s = 2$, for η)

$$[\eta]_1 \times 10^7 = 133.46\sqrt{T.M}/\alpha^2\rho^2 I(\alpha)_{(2,2)} \qquad \ldots \quad (6)$$

In Eq. (6) ρ is temperature independent and $\alpha^2 I(\alpha)_{(2,2)}$ is temperature dependent. Let η_1 and η_2 be the viscosities at temperatures T_1 and T_2 respectively. Then

$$[\eta_2/\eta_1] = (T_2/T_1)^2(\alpha_1/\alpha_2)^2[I(\alpha)_{(2,2)}]_2/[I(\alpha)_{(2,2)}]_1 \qquad \ldots \quad (7)$$

where $[I(\alpha)_{(2,2)}]_1$ and $[I(\alpha)_{(2,2)}]_2$ represent the collision integrals corresponding to α_1 and α_2 respectively. Hence by knowing the quantities η_1 and η_2 experimentally, values of A can be so adjusted that the right hand side of Eq. (7) becomes equal to $[\eta_2/\eta_1]_{expt}$. For a particular substance different experimental values of the ratio $[\eta_2/\eta_1]$ were taken and A values were found in each case. The geometric mean of the A values so obtained was taken as the true values of the constants for the substance. Once A is obtained the value of ρ can be found from Eq. (6). The arithmetic mean of all ρ values thus obtained was taken as the true value for the substance. The values of the constants thus obtained are given in Table I. For the sake of comparison the values of the constants obtained by Amdur and Mason (1958) from scattering experiments are also given in the Table I.

TABLE I

Values of the constants A and ρ on the exp-model

Substance	From Viscosity			From Scattering		
	$A \times 10^8$ ergs.	ρ in Å	Range of rigid sphere diameter r_0 in Å	$A \times 10^8$ ergs.	ρ in Å	Range of rigid sphere diameter r_0 in Å
He	0.0615	0.225	1.946—1.984	0.0618	0.220	1.3—2.3
A	5.125	0.244	3.106—3.214	5.174	0.224	2.2—3.4
N_2	1.053	0.295	3.292—3.383	2.163	2.063	2.4—3.6
O_2	1.086	0.275	3.082—3.222	—	—	
CO_2	1.149	0.328	3.654—3.843	—	—	

The potential parameters determined from viscosity and scattering data are not quite consistent.

TABLE II

Substance	T°K	$\eta \times 10^7$ g cm.sec. expt.	$\eta \times 10^7$ g/cm. sec. calculated with force constants from	
			Viscosity	Scattering
	800	3840[T]	3873	4042
	850	4000[a]	4049	4226
He	900	4154[a]	4222	4407
	950	4304[a]	4394	4584
	1000	4455[T]	4587	4764
	800	4621[v]	4677	5412
	900	4960[a]	4961	5870
	1000	5302[v]	5282	6263
A	1100	5636[a]	5626	6649
	1200	5947[v]	5948	7044
	1300	6256[a]	6272	7437
	1400	6532[a]	6601	7802
	1500	6778[v]	6900	8196
	800	3493[v]	3379	3764
	972.5	3916[e]	3856	4287
	1000	4011[v]	3929	4367
	1020.7	4017[e]	3986	4430
	1068.8	4119[e]	4108	4563
N_2	1120.2	4216[e]	4240	4710
	1166	4374[e]	4359	4838
	1220.5	4461[e]	4499	4984
	1273.2	4582[e]	4629	5134
	1500	5050[v]	5174	5728
	800	4115[a]	4131	
	1000	4720[a]	4806	
	1130	5230[e]	5240	
O_2	1166	5382[e]	5342	
	1203	5480[e]	5459	
	1278	5677[e]	5685	
	1292	5715[e]	5728	
	800	3391[v]	3375	
	900	3676[a]	3657	
	1000	3935[v]	3925	
CO_2	1100	4200[a]	4188	
	1200	4453[v]	4442	
	1300	4688[a]	4736	
	1400	4912[a]	4933	
	1500	5139[v]	5169	

[T] Trautz, M. and Zink, R. (1930).
[v] Vasilesco, V. (1945).
[e] Raw, C. J. G. and Ellis, C. P. (1958).
[e] Raw, C. J. G. and Ellis, C. P., (1959).
[a] Values obtained from the interpolation of available high temperature viscosity data.

COMPARISON WITH EXPERIMENT

(*a*) *Viscosity*

An obvious test of the success of any molecular model is its ability to reproduce various experimental data with the same set of constants. In Table II, the experimental and the calculated values of the viscosity coefficients of He, A, O_2, N_2 and CO_2 at high temperatures are given. The calculated values on the exp-model from the force-constants obtained by Amdur and Mason (1958) from scattering data are also given. It can be seen from Table II that the experimental viscosity data are reproduced much better on the exponential model with the force constants determined in the present work than with those determined from scattering data. This is due to the fact that the rigid sphere diameter range of validity of the two sets of parameters are different. Parameters from scattering data are expected to be more appropriate at still higher temperatures.

(b) *Inter-diffusion coefficient*

The binary diffusion coefficient may be written to the first approximation as (Hirschfelder *et al.*, 1954)

$$[D_{12}]_1 = 0.002628\sqrt{T^3(M_1+M_2)/2M_1M_2}/p\sigma_{12}^2\Omega_{12}^{(1,1)*} \quad \ldots \quad (8)$$

where p is the pressure in atmospheres, M_1 and M_2 are the molecular weights of the species 1 and 2 respectively. Using the values of $\sigma_{12}^2\Omega_{12}^{(1,1)*}$ as determined with the help of Eq. (4), the expression (8) for the diffusion coefficient on the exp-model becomes,

$$[D_{12}]_1 = 0.002628\sqrt{T^3(M_1+M_2)/2M_1M_2}/4p\alpha_{12}^2\rho_{12}^2 I_{(1,1)}(\alpha_{12}) \quad \ldots \quad (9)$$

The constants A_{12} and ρ_{12} for the pair 1—2 may be approximated by the use of the combination rules given by Amdur and Mason (1958)

$$1/\rho_{12} = 1/2(1/\rho_1+1/\rho_2) \quad \ldots \quad (10)$$

$$A_{12} = (A_1 \times A_2)^{\frac{1}{2}} \quad \ldots \quad (11)$$

and α_{12} is defined as before

$$\alpha_{12} = \ln (A_{12}/kT) \quad \ldots \quad (12)$$

The values of the integrals $I_{(1,1)}(\alpha_{12})$as functions of α_{12} have been tabulated by Monchick (1959).

Recently Walker and Westenberg (1958, 1959 and 1960) have measured the inter-diffusion coefficients at high temperatures for a number of gas pairs by the "point source technique." By using the combination rules, Eqs. (10) and (11), the inter-diffusion coefficients for the systems He–A, He–N_2, CO_2–N_2 and CO_2–O_2 have been calculated by us with the force constants determined from viscosity.

The results of these calculations together with the experimental values are given in Table III. Examination of the results in Table III shows that the agreement between the calculated and the experimental values of the diffusion coefficients is very poor for systems involving CO_2. This discrepancy in the case of CO_2 can be attributed to the fact that the CO_2 molecule is a much poorer approximation to spherical elastic particle than the other simple molecules and the simple combining rules valid for central force fields are not as appropriate. This has also been observed by Walker and Westenberg. Further, Mason *et al.* (1960) have pointed out that the effect of excitation or charge exchange will be important in case of high temperature diffusion and thermal diffusion in particular. Besides, multiplicity of the different interaction energy curves governing collisions should also be taken into account.

TABLE III

Calculated and experimental values of binary diffusion coefficients for system He–A, He–N_2, CO_2–N_2 and CO_2–O_2.

System	T°K	D_{12} cm²/sec. expt.	D_{12} cm²/sec. calculated with force constants from viscosity
He–A	700	3.500	3.062
	800	4.355	3.852
	900	5.338	4.692
	1000	6.1905	6.067
	1100	7.207	7.131
He–N_2	700	3.000	3.074
	800	3.828	3.864
	900	4.686	4.747
	1000	5.614	5.676
	1100	6.572	6.674
CO_2–N_2	700	0.8095	0.6232
	800	1.022	0.7794
	900	1.251	0.9506
	1000	1.486	1.134
	1100	1.724	1.345
	1200	1.937	1.544
CO_2–O_2	700	0.7696	0.6469
	800	0.9759	0.8102
	900	1.197	0.9872
	1000	1.440	1.180
	1100	1.679	1.387

The small amount of discrepancy observed in the calculated and the experimental values of the diffusion coefficients for He–A at the lower temperature can be explained by assuming that the diffusion corresponds to more penetrating collisions than other transport properties at the same temperature (Hirschfelder and Eliason, 1957) and therefore the parameters from scattering data are expected to give better agreement.

ACKNOWLEDGMENTS

The author wishes to express his thanks to Prof. B. N. Srivastava, D.Sc., F.N.I., for his valuable guidance. Thanks are also due to Dr. A. K. Barua for suggesting the problem and valuable discussions throughout the progress of the work.

REFERENCES

Amdur, I. and Ross, J., 1958, *Combustion and Flame*, **2**, 412.
Amdur, I. and Harkness, A. L., 1954, *J. Chem. Phys.*, **22**, 664.
Amdur, I. and Mason, E. A., 1954, *J. Chem. Phys.* **23**, 415.
Amdur, I. and Mason, E. A., 1954, *J. Chem. Phys.* **22**, 670.
Amdur, I. and Mason, E. A., 1955, *J. Chem. Phys.* **23**, 2268.
Amdur, I. and Mason, E. A., 1956, *J. Chem. Phys.* **25**, 624.
Amdur, I., Mason, E. A. and Jordhan, 1957, *J. Chem. Phys.* **27**, 527.
Amdur, I. and Mason, E. A., 1958, *Phys. Fluids*, **1**, 370.
Cottrell, T. L., 1956, *Disc. Faraday. Soc.*, **22**, 10.
Hirschfelder, Curtiss and Bird, 1954, Molecular Theory of Gases Liquids, (John Wiley & Sons, Inc., N.Y.)
Hirschfelder, J. O. and Eliason, E. A., 1957, *Ann. N.Y. Acad. Sci.*, **67**, 451.
Monchick, L., 1959, *Phys. Fluids*, **2**, 695.
Mason, E. A., Vanderslice, J. T. and Yos, J. M., 1960, *Phys. Fluids*, **2**, 686.
Raw, C. J. G. and Ellis, C. P., 1958, *J. Chem. Phys.*, **28**, 1198.
Raw, C. J. G. and Ellis, C. P., 1959, *J. Chem. Phys.*, **30**, 574.
Trautz, M. and Zink, R., 1930, *Ann. Physik*, **7**, 427.
Vasilesco, V., 1945, *Ann. Physique*, **20**, 292.
Walker, R. E. and Westenberg, A. A., *J.* 1958, *Chem. Phys.*, **29**, 1147.
Walker, R. E. and Westenberg, A. A., 1959, *J. Chem. Phys.*, **31**, 519.
Walker, R. E. and Westenberg, A. A., 1960, *J. Chem. Phys.*, **32**, 436.

41

AN INTERNAL COUNTER CONTROLLED LOW PRESSURE CLOUD CHAMBER

M. RAMA RAO

Saha Institute of Nuclear Physics, Calcutta

(*Received February* 15, 1961)

ABSTRACT. A low pressure internal counter controlled cloud chamber operating at a pressure of 8 cm of Hg is described. The details of the electronic circuitry for running the chamber automatically are also presented.

I. INTRODUCTION

During the early stages of work with cloud chambers, the instrument has been operated in a random fashion. In the study of rare events as in cosmic rays and other infrequent nuclear processes, the chances that an ionizing event passes through the chamber right at the instant a random expansion is initiated being very uncertain, one has to take a prohibitively large number of photographs to get any useful information, for most of the photographs will go blank. A random mode of operation, therefore, suffers from the drawback that an investigation undertaken along such lines is very uneconomical from the point of view of the large film consumed and the long time involved. Such a situation was answered for the first time by Blackett and Occhialini (1933) who, while conducting experiments on cosmic rays, evolved a new technique in which the release mechanism of the expansion cloud chamber is actuated only in the event of an ionizing particle traversing through the chamber. The technique is well known An array of Geiger counters is placed external to the cloud chamber at the top and bottom and when the charged particle under consideration traverses through all the three constituents of the assembly, the electronic counter circuits give rise to a triggering pulse within a few microseconds of the travel of the chamber by the desired ionizing particle which releases the expansion mechanism and puts a series of other electronic controls into operation thus making it possible to have the tracks automatically photographed. The vast improvement in efficiency achieved by working the cloud chamber in conjunction with Geiger counters has made this arrangement a standard practice with all present day cloud chambers which are known as counter controlled cloud chamber".

But in the investigations of low energy particles produced within the chamber, the control arrangement with the aid of external counters would be of little avail, since the particles with their short ranges are absorbed within the walls of the

chamber itself, thereby preventing the particles from reaching the counters placed outside. Under such circumstances, it would, therefore, be an appropriate choice to place the counter inside the chamber itself. Bridge *et al.* (1948) and Leighton *et al.* (1949) have tried to work with thin-walled ion chambers and Geiger counters in the sensitive volume of the chamber. But even with the conventional counters placed inside the cloud chamber, the particle could still get bsorbed aby the cathode of the counter which normally is a hollow thin copper cylinder sealed within a glass envelope. This difficulty was overcome by Hodson and Loria (1950) who first succeeded in controlling a cloud chamber by using an "open counter" in which the cathode consisted of a cylindrical arrangement of thin rods or wires, instead of the usual metal tube. Thus by using wire electrodes which defined the cathode configuration of the counter inside the chamber, it was possible to make the counter volume a part of the sensitive region of the chamber and there was no material except the filling gas itself to retard the motion of the low energy particles. They operated the cloud chamber and consequently the counter at a pressure of 1.5 atmospheres and the filling mixture used was argon saturated with ethyl alcohol vapour.

In the present work, the technique of internal counter controlled operation has been extended to very low pressures. This paper includes details of the electronic sequence circuitry for running the cloud chamber automatically, together with some preliminary results testing the working of the instrument.

II. EXPERIMENTAL ARRANGEMENT

When an ionizing event takes place within the cloud chamber, the gas inside is ionized and the electron component of the ionized gas is collected by the central wire of the proportional counter operated within the chamber at a positive high potential. The electronic counter circuits thus give rise to a triggering voltage pulse and this pulse is used to set off a sequence of events so as to make a photographic record of the tracks of the charged particles automatically.

Fig. 1 presents the block diagram of the electronic timing circuit for the expansion chamber. The events take the following sequence :

1. The counter pulses are passed through a preamplifier and then suitably amplified by means of a high gain amplifier.
2. The pulses are admitted into a discriminator circuit where pulses due to the desired events can be discriminated.
3. The discriminated pulse is employed to run a high voltage quenching circuit which removes the high voltage on the counter before the positive ions along the path of the incident particle have had time to move any appreciable distance and the track is therefore visible and undistorted even within the sensitive volume of the counter.

4. The same pulse after discrimination is utilised to open the expansion valve which goes to complete the expansion of the cloud chamber.

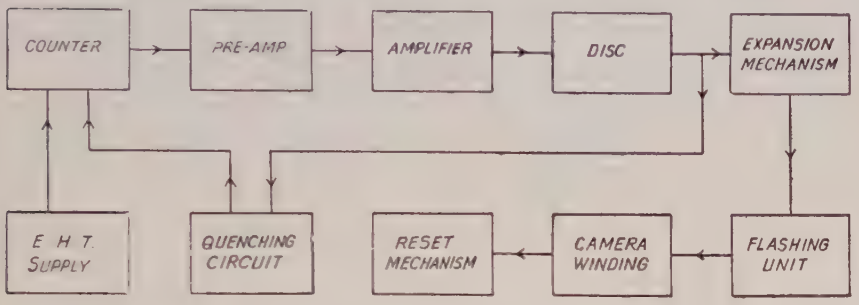

Fig. 1. Block diagram for automatic operation of the cloud chamber.

5. The flashing units are fired after a suitable delay to illuminate the tracks of droplets formed and the camera catches the photograph of the event.

6. The camera automatically winds up providing fresh film for a subsequent event.

7. The pressure in the back chamber, thereby expansion ratio, in the meantime, is automatically adjusted and the chamber kept ready for another expansion.

III. CONSTRUCTIONAL DETAILS OF THE COUNTER

The counter is mounted across the middle of the cloud chamber, the details of which have been published elsewhere (Rama Rao, 1961). The counter is 20 cms in length and 3.0 cms in diameter. The cathode assembly of the counter is defined by four rods 1 mm in diameter supported at the ends by copper rings. The anode is a 3 mil tungsten wire stretched axially with respect to the cylinder defined by the cathode assembly. The cathode supporting rings are fitted with perspex discs. To one end of the anode wire a glass bead is fused and held against a small hole at the centre of the perspex disc. The other end of the wire is taken through the centre of the perspex disc facing the previous one and is fused into a brass screw and the wire is kept straight by applying suitable tension and tightening the nut against the perspex disc. Proper care is taken to prevent any twisting of the wire while fixing up. A connecting lead is soldered to the screw and brought out through a narrow drill hole in the wall of the perspex chamber. The chamber is made leak tight at this point by applying transparent glyptal. The whole counter assembly is mounted on two rigid supports made of copper that take the form of brackets bent in the form of a right angle and screwed on firmly to the metallic flange of the chamber. Thus the cathode of the counter is kept at the ground potential by grounding the

metallic casing of the cloud chamber. The details of mounting the counter within the chamber are shown in Figs. 2 and 2a.

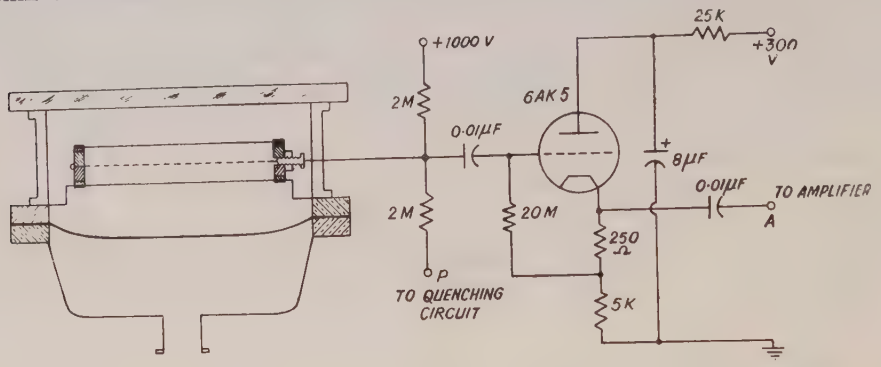

Fig. 2. Counter mounting within the chamber and cathode follower pre-amplifier.

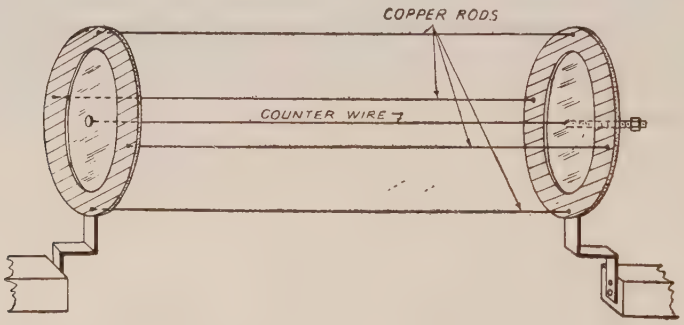

Fig. 2a. Perspective view of the counter.

IV. CHOICE OF GAS-VAPOUR FILLING

In the present set-up, the proportional counter which is incorporated within the cloud chamber is not isolated from the chamber volume by glass envelope whatsoever, but forms a part of the sensitive region of the chamber itself. Such being the case, the choice of the gas-vapour mixture filling the chamber comes up as a major consideration. The same gas-vapour composition must play the dual role of a satisfactory cloud chamber filling mixture for obtaining good tracks and at the same time a satisfactory filling for operating the counter in the proportional region.

When an ionizing particle moves through the gas of the counter, it gives rise to a number of electrons and an equal number of positive ions along its track. The electrons created by the primary ionizing particle can be drawn towards the anode which is maintained at a positive potential. If the attractive voltage acting on the electrons is suitably adjusted, the electrons can be drawn into the near vicinity of the wire and there they enter a region in which the field strength

rapidly increases in magnitude. Thus in traversing through a short distance, the electrons originally produced along the track now acquire between collisions with atoms and molecules sufficient kinetic energy to result in further multiplication of ions due to secondaries which remain proportional to the initial ionization as long as the counter is operated in the proportional region. It can thus be seen that such gas multiplication is possible only when the electrons remain freely mobile and the gas-vapour composition does not exhibit appreciable electron affinity. For this reason, oxygen and water vapour both of which have great affinity for electron attachment had to be excluded from the chamber filling. A filling of commercial argon (99.8% purity, oxygen-free) and isoamyl alcohol has been found to be a satisfactory mixture for operating the chamber in the region of 5 cms of Hg. Detailed investigations on the choice of gas-vapour composition had been undertaken and the results were communicated in an earlier paper (Rama Rao, 1961). The same composition is now found to go well with the counter operating in the proportional region.

V. INTERNAL COUNTER OPERATION FOR EXPANDING THE CLOUD CHAMBER

The anode of the counter is operated at a positive high potential while the cathode rods are earthed. When an ionizing particle passes through the cloud chamber and therefore the counter, the gas inside is ionized leaving positive ions and electrons. Since pure argon has been used as the permanent gas in the cloud chamber, there is very little tendency for the electrons to attach themselves to the gas molecules to form negative ions. Thus all the electrons are now accelerated towards the central anode wire of the counter and get collected there. The negative pulse collected by the wire is amplified by a high gain linear amplifier and is utilised in bringing about the expansion of the cloud chamber.

The collection of electrons by the counter is completed within an interval of a few microseconds. It is known that the mobility of electrons is much higher than that of the heavier ions. This leads to the advantage that if the voltage pulse due to the electron collection triggers the expansion of the cloud chamber, the slow positive ions, which have not had time to diffuse to any appreciable extent, would act as condensation nuclei for the vapour and enable to obtain a photograph of the tracks that are responsible for triggering the chamber.

The present counter with its dimensions mentioned earlier has a suitable proportional region over the range 850-1000 volts when operated at pressures of 8 cms of Hg. With this set of operating conditions it has been found possible to reproduce the pulse sizes in the counter over a period of 2 to 3 days. Thereafter, the pulse size diminished steadily owing to change in the composition of the gas-vapour mixture as a result of slow diffusion of air into the chamber through the rubber gaskets and also due to release of oxygen and moisture from the walls

of the perspex chamber. It was thus found necessary to exhaust the chamber once in 3 days and refill the chamber to have a reproducible counter performance.

VI. ELECTRONIC CIRCUITRY FOR COUNTER OPERATION OF THE CLOUD CHAMBER

It is proposed to discuss here in some details the functions and performance of the different electronic circuits used in the operation of the instrument.

a) *Amplifier and Discriminator*

The negative pulses from the anode of the counter are taken through a cathode follower pre-amplifier to the main amplifier. The pre-amplifier (Fig. 2) is placed close to the counter and this is necessary because the grid of the input stage must be as close as possible to the electrical detector in order to keep capacitance at a minimum. Shielded cables of short lengths have been used to carry the pulses from the counter to the input of the pre-amplifier. The output from the pre-amplifier is fed to the input stage of the main amplifier at the point A.

The pulse amplifier used (Fig. 3) has two three-tube feed back loops each with a gain of 100. Thus the total gain is 10^4 and can be varied by means of coarse

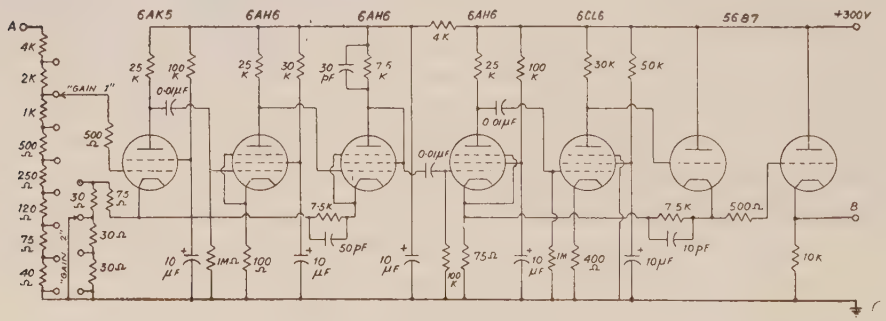

Fig. 3. Amplifier.

and fine controls. The measured band width of the amplifier is roughly 1 cm. It is identical with Model 100 pulse amplifier described by Elmore and Sands (1949) with the exception that equivalent miniature tubes have been used to derive the advantages of their low interelectrode capacitances. Shielded coaxial cables have been used to carry the pulses from the pre-amplifier to the input of the main amplifier and sufficient care has been taken to shield the amplifier adequately in order to avoid pick-up of transient electrical disturbances.

The positive output pulses from the amplifier are taken through a cathode follower and are fed at the point B to drive a voltage discriminator circuit (Fig. 4).

The bias voltage of the discriminator is adjusted by setting the potentiometer so that the circuit triggers for input pulses of pre-determined amplitudes. Out-

put pulses of approximately 80 volts amplitude are taken from the plate of the second tube of the discriminator and are used to drive the voltage quenching circuit and the sequence circuit.

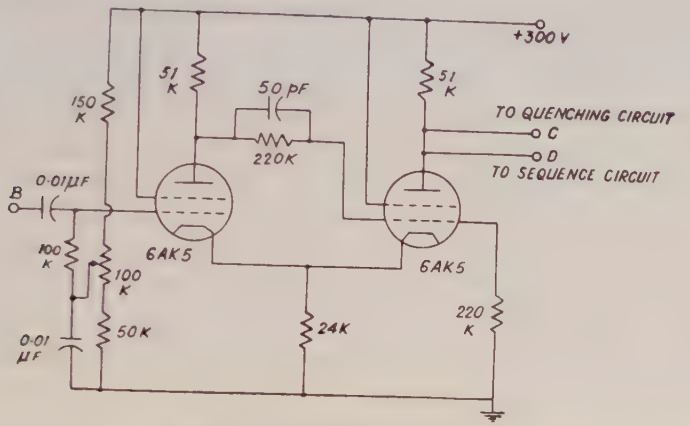

Fig. 4. Discriminator circuit.

b) *High voltage quenching circuit*

It is necessary to remove the high voltage on the proportional counter as soon after the collection of the electron component of the ionization event as possible so that the positive ions have had little time to disperse in the gas medium under the action of the strong electric field in the vicinity of the counter, which other-wise would result in broadening and distortion of the tracks. A portion of the track is also lost in the sensitive volume of the counter. The lowering of voltage on the counter much below the operating point is achieved by using a quenching circuit in the voltage supply of the proportional counter.

The operation of the voltage quenching circuit is explained with reference to Fig. 5 and Fig. 2. The discriminator pulse is taken to point C of the voltage

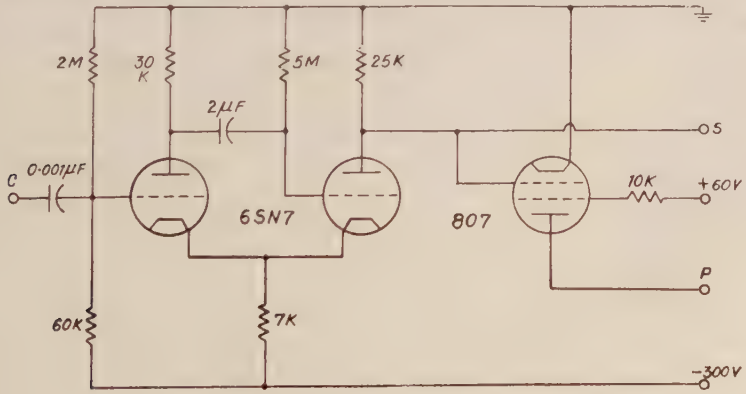

Fig. 5. High voltage quenching circuit.

quenching circuit which is composed of a cathode coupled multivibrator circuit and a 'voltage quenching tube'. Type 6SN7 tube is used for the multivibrator part of the circuit and type 807 is the quenching tube. The plate point of 807 is tied to the anode of the counter through a 2MΩ resistor. The plate point of the conducting half of 6SN7 is connected to the grid of 807 tube so that the grid of 807 is maintained at a high negative potential with respect to the cathode and the tube does not draw any current. Therefore, at the start the full voltage applied on the counter also resides on the plate of 807. Now when the multivibrator circuit is triggered by the incoming pulse, the conducting section of 6SN7 tube becomes non-conducting and the grid of 807 is raised to zero potential. The 807 tube now conducts and there is a voltage drop across the plate load of 807 which is experienced by the counter anode. The voltage on the counter is thus lowered from a positive high voltage to a few volts in a very short interval of time and the voltage on the counter remains lowered until the multivibrator recovers to its normal state, determined by the CR value of the circuit which is of the order of a few seconds. By suitably adjusting this delay, the voltage on the counter has been kept lowered until the cloud chamber expansion is completed and photographs of tracks have been obtained.

(c) *Sequence control circuit*

The sequence circuit (Fig. 6) includes the chamber expansion device and other auxiliary time sequence control circuits for the flashing of lamps, winding the camera, and resetting the chamber after every cycle of operation.

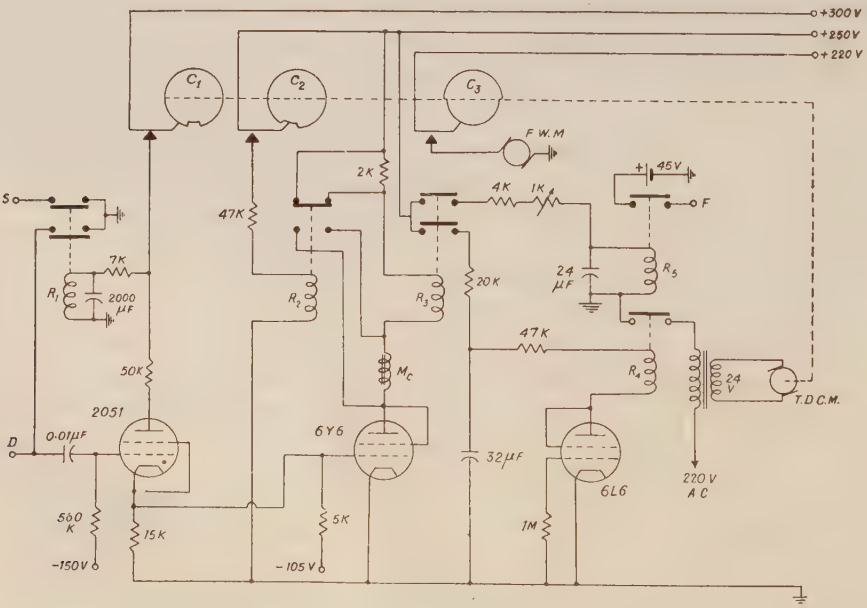

Fig. 6. Timing sequence circuit.

The magnet coil M_c of the high vacuum magnetic valve which brings about the expansion of the chamber is included in the plate circuit of 6Y6 tube. The magnet is of the type that normally remains closed under gravity. The grid bias on 6Y6 tube is initially maintained sufficiently negative such that the tube does not conduct and hence the magnet is not energized. The grid of 6Y6 tube is tied to the cathode point of the thyratron tube 2051. When the voltage pulse from the discriminator is fed to the grid of 2051, the tube fires and the voltage developed across the cathode resistor of 2051 raises the grid potential of 6Y6 to zero volt and makes 6Y6 conducting. The plate draws current and the magnet coil is energized, thus opening the magnet valve so as to expand the chamber.

R_3 is a relay operating in series with the magnet coil. Normally the relay is in the off-position and is energized along with the magnet coil of the main expansion magnet. With the help of relay R_3, two circuits are operated with suitable delays introduced in their paths. The circuit operated from one set of contact points is intended for running flashing units and the one from the other set drives a time delay cam motor (T.D.C.M.).

The action of T.D.C.M. can be understood as follows : When the relay R_3 is energized, H.T. is supplied to the plate of 6L6 thus making it conducting. The relay R_4 which is in the plate circuit is now energized and the primary circuit of the transformer which is connected across the contact points of this relay is completed. A 24 volt motor is operated from the secondary of the transformer and the speed of the motor is cut down by suitable reduction gear system. Cams C_1, C_2, C_3 are mounted axially on the shaft of the motor. The cams are made of small circular perspex discs. Shallow slots of varying widths are cut on the periphery of these discs. Three contact switches are mounted on an insulated base plate close to the discs such that the switches sweep out the periphery of the perspex discs as the motor shaft carrying these discs begins to rotate. When one of the prongs of the switches falls into the slot, the contact breaks and the corresponding circuit operated by this particular switch is disconnected. Thus the elevated portions on the three cams determine the time scale for which a particular circuit is held in operation. A magnified picture of the time delay cams is presented in Fig. 7.

When once the thyratron is fired and the sequence circuit is put into operation, the cam begins to rotate until the switch on cam C_1 interrupts the plate voltage of the thyratron tube. The time for a complete revolution is set at 3 minutes and this gives the operation cycle of the cloud chamber. It can thus be seen that the magnet coil of the expansion magnet also remains energized for the whole time the thyratron is in the conducting state. But we wish to return the magnet valve to its normal condition as soon after photography of the ionizing event as possible so as to isolate the back chamber from the vacuum ballast and raise the pressure in the back chamber to the present value by admitting air through an

auxiliary air admittance valve, details of which have been described in an earlier paper (Rama Rao, 1961). The magnet valve is returned to its normal position

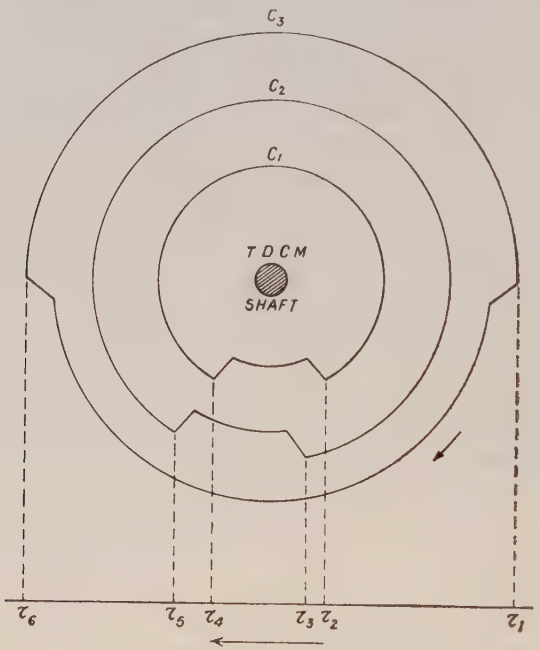

Fig. 7. Magnified diagram of the time delay cams.

by short circuiting the magnet coil. This is done with the help of relay R_2 which operates through the contact switch mounted on Cam C_2. The slot on cam C_2 is slightly displaced with respect to the one on cam C_1 so that as the cam rotates the switch on cam C_2 comes into operation a little while after the expansion is complete. As soon as the relay R_2 is pulled down, the magnet coil is short circuited thus shutting the valve and a 2K resistance appears in series with the relay coil R_3 keeping the total plate load of 6Y6 unaltered. The magnet coil is thus short circuited for the complete cycle, as long as the contact switch on C_2 is closed which is released only after the contact switch on C_1 is opened.

d) *Flashing circuit*

The tracks of ionizing particles are photographed under strong illumination which lasts momentarily. The illumination is provided by two Mazda flashing lamps F.A.2 with a rating of 2500 VDC and 500 joules dissipation. The circuit for operating these tubes is showing in Fig. 8.

Along with the expansion of the magnet, the relay R_3 is energized and through one set of contact points of the relay R_3 voltage is applied to the relay R_5 which is energized after a delay determined by the CR value in the circuit. Closing of the relay contacts gives rise to a positive pulse from a battery of 45 volts which is

fed to the point F to trigger a cathode coupled multivibrator (Fig. 8). The negative rectangular pulse taken from the plate of the first half of 6SN7 tube is dif-

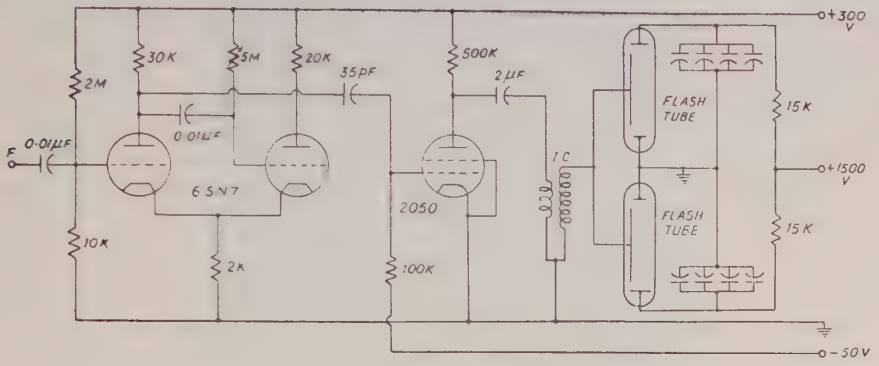

Fig. 8. Flashing unit.

ferentiated by the 35pf and 100KΩ net work. The positive spike of the differentiated pulse is utilized to fire the thyratron tube 2050. The triggering action of 2050 can be delayed with respect to the input pulse at F by 5 MΩ potentiometer. When the switching action of the thyratron takes place, a 2μf condenser which is previously charged to 300V is now discharged producing a current surge in the primary of the Ignition coil (I.C.). The high voltage pulse developed across the secondary which is of the order of several KV is applied to the trigger electrode of the flash tubes. Two banks of condensers, each 64μf, connected across the flash lamps and charged to 1500 volts D.C., get discharged through the tubes owing to the breakdown of the gap between the electrodes as a result of the sudden rise in the electric field and thus an intense burst of light is obtained.

e) *Photography and film winding*

The camera for taking stereoscopic pictures is mounted vertically above the cloud chamber. The camera is of the open shutter type and hence the cloud chamber had to be operated in a dark room.

After the event has been photographed, the film is wound up and set ready for the next photograph. This is done by a slow motion motor (F.W.M.) which is kept in motion by the operation of the contact switch on cam C_3. The time for which the motor is running to wind up the exposed portion of the film is determined by the length of the slot on the cam C_3.

f) *Reset mechanism*

When once the thyratron of the sequence circuit is fired and the sequence circuit put into operation, the grid loses its control on the performance of 2051 tube and the tube remains conducting and consequently the associated circuits on, until the switch on cam C_1 interrupts the plate voltage on 2051. As the cam

rotates after a complete cycle of operations of the sequence when the slotted portion faces the switch on C_1, the voltage on 2051 is removed, rendering it non-conducting and thus the rest of the circuit is thrown out of action. The circuit has to be set ready for a subsequent operation by restoring the voltage on the plate of 2051. This is achieved as follows:

As soon as the switch contact on cam C_1 is broken, 2051 is extinguished and hence 6Y6 becomes non-conducting, de-energising the relay R_3. Though the plate supply for 6L6 tube which it gets through the relay contacts of R_3 is cut off, the charge accumulated by the 32μf condenser supplies the voltage for the relay coil R_5 and holds it in the on-position and consequently the T.D.C. motor running. This continued operation of the motor for a little while after the main source of supply voltage is cut off overshoots the slotted portion of the cam C_1 so that the contact of the switch on C_1 is re-established and occupies the position indicated in (Fig. 6). The plate voltage on 2051 is thus restored and the tube is ready for triggering on the arrival of a fresh pulse at the grid of the tube.

g) *Spurious operation of the chamber*

It was occasionally detected in a few blank operations that at the time of establishing the switch contact on cam C_1 after a complete cycle of operations, due to faulty contact, a spark at the contact point was a source of disturbance which after having been picked up and amplified is fed to the grid of 2051, thus driving the circuit and giving a fake expansion without a real pulse from the counter being fed.

This was avoided by cleaning the contacts regularly and also by ensuing smooth contacts by adjusting the gap between the contact points. Additional precaution was taken to ground the grid of 2051 during the time the switch contact was being established. This can be understood by referring to the operation of relay R_1 in (Fig. 6). When the contact switch is in the slotted portion of cam C_1, the relay R_1 is disengaged and the input to the grid of 2051 is grounded through a pair of contact points of relay R_1. When the contact switch on cam C_1 is being pulled out of the slot and voltage on plate of 2051 restored, the relay R_1 is energized but slowly owing to the high value of the capacitor, 2000μf, thus the grounding of the input to 2051 is released only after firm contact of the C_1 cam-switch is established.

For the time the grid of 2051 is grounded, the grid of 807 tube is also kept at ground potential by connecting the grid of 807 at the contact point S of relay R_1. This brings about the removal of voltage on the counter once again thereby avoiding the production of fresh ionization by discharges in the counter.

VII. RESULTS AND DISCUSSION

A preliminary testing of the set-up has been made by initiating the expansion of the cloud chamber using α-pulses picked up by the counter. Fig. 9 shows a photograph of α-tracks obtained at 8 cm of Hg.

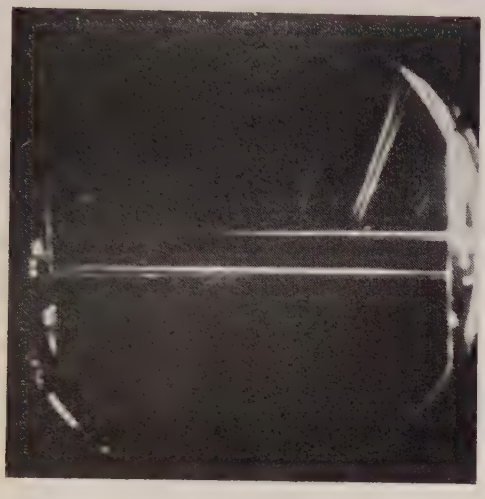

Fig. 9. Photograph of α-tracks obtained at 8 cms of Hg using argon and iso amayl alcohol as filling mixture

It may be mentioned here that the quality of tracks mainly depends upon the diffusion of ions. The width of the track is a function of the speed of expansion which is defined as the time elapsed between the moment the particle passes through the counter and the achievement of the expansion of the chamber. The time taken by the magnet to open fully is the predominant factor for obtaining sharp tracks as the delays introduced in the electronic circuit being of negligible order. The magnetic valve used in the present experiment is a high speed expansion valve and a rough estimate shows that it is of the order 5 m.sec.

ACKNOWLEDGMENTS

The author is indebted to Prof. B. D. Nag Chaudhuri, Director of the Institute, for his constant guidance and encouragement. The author is grateful to Prof. D. N. Kundu for his keen interest and valuable discussions.

REFERENCES

Blackett, P. M. S. and Occhialini, G. P. S., 1933, *Proc. Roy. Soc.*, **139**, 699.
Bridge, H. S., Hazen, W. E., Rossi, B. and Williams, R. W., 1948, *Phys. Rev.*, **74**, 1083.
Elmore, W. C. and Sands, M., *Electronics* (McGraw-Hill Book Company, Inc., New York, 1949), National Nuclear Energy Series, V-1.
Hodson, A. L., Loria, A. and Ryder, N. V., 1950, *Phil. Mag.*, **41**, 826.
Leighton, R. B., Anderson, C. D. and Sheriff, A., 1949 *Phys. Rev.*, **75**, 1432.
Rama Rao, M., 1961, *Ind. J. Phys.*, **35**, 92.

Letters to the Editor

The Board of Editors will not hold itself responsible for opinions expressed in the letters published in this section. The notes containing reports of new work communicated for this section should not contain many figures and should not exceed 500 words in length. The contributions must reach the Assistant Editor not later than the 15th of the second month preceding that of the issue in which the letter is to appear. No proof will be sent to the authors.

4

THE CRYSTAL STRUCTURE OF BENZALAZINE

U. C. SINHA

Physics Department, Allahabad University,
Allahabad, India

(*Received April* 22, 1961)

In an earlier communication (Sinha, 1959), the space group of benzalazine along with other crystallograhic data has already been published. However, the axial lengths were redetermined from high angle Bragg reflections in Weissenberg photographs by the method of Lipson and Farquhar (1946), after necessary correction for film-shrinkage error, etc. The revised values of the axial parameters thus obtained are

$$\left.\begin{aligned} a_0 &= 13.09\ \text{Å} \\ b_0 &= 11.76\ \text{Å} \\ c_0 &= 7.62\ \text{Å} \end{aligned}\right\} \quad \alpha = \beta = \gamma = 90°,$$

the space-group being $D^{12}{}_{2h}$—Pbcn, containing four molecules per unit cell. This space-group containing a centre of symmetry has eight equivalent points in the unit cell. The structural formula of the molecule of benzalazine is C_6H_5 . CH : N. N : CH. C_6H_5. It shows that the molecule has a centre of symmetry. This indicates that the centre of the N N bond must lie at the centre of symmetry which has been chosen to be the origin of the coordinates.

The relative intensities of the reflections *hko*, *hol* and *okl* were measured by photographic method, absolute values were obtained by comparing these with the known absolute values of F_{hkl} of aluminium and hence the structure factors were obtained.

The intensity of (002) diffuse reflection suggested that the orientation of the benzene ring of the molecule would be near about (001) plane. In addition, by a consideration of the high intensity (*hko*) reflections of higher indices using the method adopted by Robertson and White (1945) for coronane, the approximate co-ordinates (x, y) were obtained after giving a few trials. Using these trial coordinates, the phases of the structure factors were calculated for computing the electron density projection $\rho(x\ y\ o)$ along [001] with the observed values of the structure factors F(*hko*). The preliminary structure thus obtained was refined by three successive [001] axis Fourier projections to give the more and more accurate values of x and y co-ordinates. Trial z-coordinates were worked out from the standard bond lengths of the molecule in order to calculate the phases of (*hol*) reflections. The z-coordinates were finally determined from the second electron density projection $\rho(xoz)$ obtained with the observed values of F(*hol*). The co-ordinates of the benzalazine molecule are given in Table I.

TABLE I

Atoms	X in Å	Y in Å	Z in Å
N	0.69_4	0.12_7	$+0.07$
C_1	1.23_9	1.00_3	-0.32_6
C_2	2.68_3	1.26_8	-0.16_5
C_3	3.27_2	2.40_6	-0.66
C_4	4.60_3	2.66_5	-0.50_8
C_5	5.40	1.76_4	$+0.14_6$
C_6	4.84_3	0.62_7	$+0.63_5$
C_7	3.49_5	0.36_2	$+0.49$

The reliability index factor

$$R = \frac{\Sigma|(|F_o| - |F_c|)|}{\Sigma|F_o|}$$

came out to be 0.20 for F(*hko*) reflections and 0.24 for F(*hol*) reflections. In the calculation of the structure factors, the atomic scattering factors for carbon and nitrogen (McWeeny, 1951) have been used after imposing an isotropic B-factor of 3.00×10^{-16}.

The structure of benzalazine is being further refined by the method of difference synthesis and other standard methods and the detailed results will be published in near future.

The author wishes to express his gratitude to Prof. K. Banerjee, Director, Indian Association for the Cultivation of Science, Jadavpur, Calcutta, for his kind interest throughout the progress of this work and to Dr. S. C. Chakravarty for his valuable advice and help and to the Government of India, Ministry of Education, for financial assistance.

REFERENCES

Lipson, H and Farquhar, M. C. M., 1946, *Proc. Phys. Soc.*, **58**, 200.
McWeeny, R., 1951, *Acta Cryst.*, **4**, 513.
Robertson, J. M. and White, J. C., 1945, *J. Chem. Soc.*, p.607.
Sinha, U. C., 1959, *Bull Nat. Inst. Sci. India*, No. **14**, 107.

IMPORTANT PUBLICATIONS

The following special publications of the Indian Association for the Cultivation of Science, Jadavpur, Calcutta, are available at the prices shown against each of them:—

TITLE	AUTHOR	PRICE
Magnetism ... Report of the Symposium on Magnetism		Rs. 7 0 0
Iron Ores of India	... Dr. M. S. Krishnan	5 0 0
Earthquakes in the Himalayan Region	... Dr. S. K. Banerji	3 0 0
Methods in Scientific Research	.. Sir E. J. Russell	0 6 0
The Origin of the Planets	.. Sir James H. Jeans	0 6 0
Active Nitrogen— A New Theory.	.. Prof. S. K. Mitra	2 8 0
Theory of Valency and the Structure of Chemical Compounds.	.. Prof. P. Ray	3 0 0
Petroleum Resources of India	.. D. N. Wadia	2 8 0
The Role of the Electrical Double-layer in the Electro-Chemistry of Colloids.	.. J. N. Mukherjee	1 12 0
The Earth's Magnetism and its Changes	.. Prof. S. Chapman	1 0 0
Distribution of Anthocyanins	.. Robert Robinson	1 4 0
Lapinone, A New Antimalarial	.. Louis F. Fieser	1 0 0
Catalysts in Polymerization Reactions	.. H. Mark	1 8 0
Constitutional Problems Concerning Vat Dyes.	.. Dr. K. Venkataraman	1 0 0
Non-Aqueous Titration	.. Santi R. Palit, Mihir Nath Das and G. R. Somayajulu	3 0 0
Garnets and their Role in Nature	.. Sir Lewis L. Fermor	2 8 0

A discount of 25% is allowed to Booksellers and Agents.

NOTICE

No claims will be allowed for copies of journal lost in the mail or otherwise unless such claims are received within 4 months of the date of issue.

RATES OF ADVERTISEMENTS

1. Ordinary pages:
   - Full page .. .. Rs. 50/- per insertion
   - Half page .. .. Rs. 28/- per insertion
2. Pages facing 1st inside cover, 2nd inside cover and first and last page of book matter:
   - Full page .. .. Rs. 55/- per insertion
   - Half page .. .. Rs. 30/- per insertion
3. Cover pages .. .. by negotiation

25% commissions are allowed to *bona fide* publicity agents securing orders for advertisements.

CONTENTS

Indian Journal of Physics Vol. 35, No. 7 July, 1961

PRINTED BY KALIPADA MUKHERJEE, EKA PRESS, 204/1, B. T. ROAD, CALCUTTA-35
PUBLISHED BY THE REGISTRAR, INDIAN ASSOCIATION FOR THE CULTIVATION OF SCIENCE
2 & 3, LADY WILLINGDON ROAD, CALCUTTA-32